



1 The enigmatic curvature of Central Iberia and its puzzling kinematics

2 Daniel Pastor-Galán^{1,2,3}, Gabriel Gutiérrez-Alonso^{4,5}, Arlo B. Weil⁶

3 ¹Frontier Research Institute for Interdisciplinary Sciences, Tohoku University

4 ²Department of Earth Science, Tohoku University

5 ³Center for Northeast Asian Studies, Tohoku University, 41 Kawauchi, Aoba-ku, Sendai, 980-
6 8576, Japan. pastor.galan.daniel.a8@tohoku.ac.jp

7 ⁴Dept. of Geology. Faculty of Sciences. University of Salamanca. Plaza de la Merced s/n.
8 38007, Salamanca (Spain). gabi@usal.es

9 ⁵Geology and Geography Department, Tomsk State University, Lenin Street, 36, Tomsk 634050
10 Russia

11 ⁶Department of Geology, Bryn Mawr College, PA, USA 19010

12 Abstract

13 The collision between Gondwana and Laurussia that formed the latest supercontinent,
14 Pangea, occurred during Devonian to Early Permian times and resulted in large-scale orogeny
15 that today transects Europe, northwest Africa and eastern North America. This orogen is
16 characterized by an 'S' shape corrugated geometry in Iberia. The northern curve of the
17 corrugation is the well known and studied Cantabrian (or Ibero-Armorican) Orocline and is
18 convex to the east and towards the hinterland. Largely ignored for decades, the geometry and
19 kinematics of the southern curvature, known as the Central Iberian curve, are still ambiguous
20 and hotly debated. Despite the paucity of data, the enigmatic Central Iberian curvature has
21 inspired a variety of kinematic models that attempt to explain its formation with little consensus.
22 This paper presents the advances and milestones in our understanding of the geometry and
23 kinematics of the Central Iberian curve from the last decade, with particular attention to
24 structural and paleomagnetic studies.

25 When combined, the currently available datasets suggest that the Central Iberian curve
26 did not undergo regional differential vertical-axis rotations during or after the latest stages of the
27 Variscan orogeny, and did not form as the consequence of a single process. Instead, its core is
28 likely a primary curve (i.e. inherited from previous physiographic features of the crust) whereas
29 the curvature in areas outside the core are dominated by folding interference during the
30 Variscan orogeny or more recent Cenozoic (Alpine) tectonics.



31 **Keywords**

32 **Central Iberia Curve, Variscan orogen, Iberia, Cantabrian Orocline, Curved orogens,**

33 **Pangea**



34 1 Introduction

35 Mountain belt systems are the most striking product of plate tectonics. In addition to their
36 astonishing visual effect, marking the locations where ancient and modern plates collided,
37 orogenic belts often preserve a variety of rocks that have the potential to illuminate the entirety
38 of the systems pre- and syn-orogenic history. One of the most striking characteristics of the
39 majority of Earth's orogens are their curvature in plan-view (e.g. van der Voo, 2004; Marshak,
40 2004; Rosenbaum, 2014). The degree of orogenic curvature may range from a few degrees of
41 deflection in structural trend (e.g. Kopet Dag, Iran), to 180° of arc curvature (e.g. Kazakhstan arc
42 and the Carpathians). The kinematics, structural and geodynamic implications of these systems
43 are as varied as their geometries (Marshak, 2004; Weil and Sussman, 2004; Johnston et al.,
44 2013). For example, some orogenic curvatures are hypothesized to be the consequence of
45 physiographic features of the basement that pre-date orogen formation, such as irregular basin
46 architectures or plate margin salients and recesses (e.g. Jura mountains, Hindle et al., 2000),
47 which then control the growth geometry of the ensuing orogen. These systems are known as
48 primary arcs and reflect pre-orogenic geometries and show no significant or systematic vertical-
49 axis rotations along their structural length. On the other hand, oroclinal, as classically defined
50 by Carey in 1956, involve systematic differential vertical-axis rotations subsequent to initial
51 orogenic shortening: different sectors of an orogen rotate with variable magnitudes or in
52 opposite directions (e.g. Li et al., 2012). Rotations in Oroclines may occur at a range of scales,
53 from thrust emplacement at upper crustal levels (e.g. Izquierdo-Llavall et al., 2018), up to a
54 lithospheric-scale vertical-axis folding (e.g. Li et al., 2018). They can occur as single curves (e.g.
55 Maffione et al., 2009), coupled curves (Johnston, 2001), or in trains of curves (Li and
56 Rosenbaum, 2014). Oroclines can form during the main orogenic building event, known as
57 progressive oroclinal (Johnston et al., 2013; e.g., the Wyoming salient, Yonkee and Weil, 2010,
58 and Weil et al., 2010) or in a subsequent tectonic pulse, so-called secondary oroclinal (Weil
59 and Sussman, 2004). Understanding the kinematics and mechanisms of curvature formation in
60 mountain belts is a critical step to understanding orogenesis in 4D and to evaluate their
61 geodynamic consequences and paleogeographic implications.

62 The Variscan-Alleghanian orogeny resulted in the suturing of Gondwana and Laurussia
63 during Devonian-Carboniferous times, and ultimately led to the formation of the supercontinent,
64 Pangea. This long and sinuous orogen runs for >8000 km along strike and is ca. 1000 km wide,
65 transecting across Europe, to northwest Africa and into eastern North America. The final stages
66 of Pangea amalgamation (e.g. Nance et al., 2010) modified the Western Europe sector of the



67 belt into its characteristic sinuous shape, which today traces at least one, and perhaps four arcs
68 from Poland to Brittany, and then across the Bay of Biscay (Cantabrian Sea) into Iberia, where
69 the system is today truncated by the Betic Alpine orogeny in southeast Iberia (Fig. 1; e.g. Weil
70 et al., 2013). The southern truncation of the Variscan in Europe hinders a precise correlation
71 with equivalent age outcrops in NW Africa.

72 Within the Iberian Peninsula, the orogen is characterized by two large-scale curves (Fig.
73 2): (1) to the north is the well studied and nearly 180° secondary orocline, the Cantabrian (a.k.a.
74 Ibero-Armorican) Orocline, which buckled a segment of the Variscan belt from ~315 to ~290 Ma
75 (e.g. Weil et al., 2019 and references therein); and (2) to the south is a curve with disputed
76 magnitude and kinematics, and is usually referred to as the Central Iberian curve/orocline or
77 Castillian bend (Martínez-Catalán et al., 2015). Though there remains tremendous uncertainty
78 on the geometry and kinematics of the Central Iberia curve, multiple hypotheses exist as to its
79 nature, and disagreements continue on its importance in the tectonic evolution of Europe during
80 the waning stages of Paleozoic global supercontinent construction. The diversity of author's
81 interpretations of the Central Iberian curve range from a nonexistent structure (Dias et al.,
82 2016), to being one of the most important pieces to our understand of the late Carboniferous
83 and Permian geodynamics of the Iberian Variscan system (e.g. Martínez-Catalán et al., 2011;
84 2014).

85 This paper reviews the most recent advances on the geometry and kinematics of the
86 Central Iberia curve, synthesizing what we know and what we don't, and ending with a
87 discussion of the main unsolved issues. We hope that this paper fosters novel studies that will
88 lead to a better understanding of when and which mechanisms acted in the aftermath of the
89 Variscan-Alleghanian orogeny.

90 2 The long and winding orogen

91 The Variscan (Europe-NW Africa)-Alleghanian (North America) orogeny is a continental-
92 scale tectonic system (1000 km wide and 8000 km long) that sutured Gondwana and Laurussia
93 together, forming the supercontinent Pangea (e.g. Domeier and Torsvik, 2014; Edel et al., 2018;
94 Pastor-Galán et al., 2019a). The fragments of this system are now dispersed over three
95 continents, Europe, Africa and North America due to the Mesozoic break-up of Pangea (Buiter
96 and Torsvik, 2014; Keppie, 2015). This orogen formed as a consequence of a long and
97 protracted tectonic history that involved several different events, from initial convergence (ca.
98 420 Ma; e.g. Franke et al., 2017), to the consumption of multiple putative oceanic tracts and/or
99 basins that existed between Gondwana and Laurussia (ca. 280 Ma; e.g. Kirsch et al., 2012).



100 The Variscan-Alleghanian orogen itself represents the closing of at least one major ocean, the
101 Rheic (e.g. Nance et al., 2010), whose axial ridge likely failed or subducted at ca. 395 Ma along
102 its paleo-northern margin (e.g. Woodcock et al., 2007; Gutiérrez-Alonso et al., 2008a). Perhaps
103 the orogeny involved other large oceans (Stampfli and Borel, 2002; Franke et al., 2017; 2019),
104 but most surely involved several minor seaways and basins that existed between Gondwana,
105 Laurussia, and several intervening micro-continents (e.g. Azor et al., 2008, Dallmeyer et al.,
106 1997; Kroner and Romer, 2013; Díez-Fernández et al., 2016; Pérez-Cáceres et al., 2017). The
107 final continent-continent collision began after closure of all oceans and intervening seaways.
108 The commencement of this deformation was diachronistic and became progressively younger
109 westwards (in present-day coordinates): with Devonian continent-continent collisions along the
110 eastern boundary, progressing to earliest Permian ages in the westernmost sector (McWilliams
111 et al., 2013; Chopin et al., 2014; López-Carmona et al., 2014; Franke et al., 2017).

112 The present-day geometry of the Variscan-Alleghanian systems has a contorted trace
113 (Fig. 1). In Europe, from east to west, the trend starts with a prominent curve around the
114 Bohemian massif (e.g. Tait et al., 1996), followed by a deflection in the Ardennes-Bravant (e.g.
115 Zegers et al., 2003). In Brittany the outer curvature of the Cantabrian or Ibero-Armorican
116 orocline begins (e.g. van der Voo et al., 1997), and wraps nearly 180° around across the Bay of
117 Biscay as it turns in NW Iberia. The Central Iberian curve marks the final concave to the west
118 curve (in present-day coordinates) and is the focus of this paper (e.g. Aerden, 2004; Martínez
119 Catalán, 2011; Shaw et al., 2012). The orogen continues in North America where, from north to
120 south, it has salients and recesses that undulate back and forth from Atlantic Maritime Canada
121 (e.g. O'Brien, 2012) down along the Pennsylvanian and Alabama curves (e.g. Thomas, 1977).

122 Interpretation on the origin of these curvatures varies widely. The curvatures in North
123 America are argued to be the result of a preexisting irregular margin of Laurentia due to the
124 break-up of the Rodinia supercontinent, which resulted in the formation of orogenic salients and
125 recesses during subsequent Appalachian collision (e.g. Rankin, 1976; Thomas, 1977, 2004). In
126 this case, vertical-axis rotations affected only the upper crustal levels during orogenesis (e.g.
127 Marshak, 1988; Bayona et al., 2003; Hnat and van der Pluijm, 2011). In Europe, the Bohemian
128 and Ardennes-Bravant massif curvatures have poor kinematic constraints. In the Bohemian
129 Massif, some suggest secondary rotations that formed an orocline (Tait et al., 1996), while
130 others suggest little to no vertical-axis rotations and a primary arc (Chopin et al., 2012). The
131 Ardennes-Bravant Massif record some vertical-axis-rotations (e.g. Molina-Garza and
132 Zeijderveld, 1996), but it is unclear if these are a response to progressive or secondary oroclinal
133 bending, or whether rotations only affected the upper crust. The most outstanding example of



134 Variscan-Alleghanian orogen curvature is exposed in the Iberian Massif, with the Cantabrian
135 Orocline and the coupled curvature of Central Iberia.

136 2.1 Two of us: The Variscan orogen in Iberia

137 The western half of the Iberian Peninsula constitutes the Iberian massif, one of the
138 largest exposures of the Variscan orogen and the only place that contains an almost continuous
139 cross section of the orogen (Fig. 2; e.g. Lotze 1945, Julivert 1974, Pérez-Estaún et al., 1991;
140 Ayarza et al., 1998; Simancas et al., 2003; Ribeiro et al. 2007, Martínez Catalán et al., 2014,
141 2019). The majority of the Iberian Massif contains Gondwanan affinity rocks (e.g. Murphy et al.,
142 2008; Pastor-Galán et al., 2013a; Gutiérrez-Marco et al., 2017) and likely represents a proximal
143 piece of the Gondwana margin until its final amalgamation with Pangea (e.g. Pastor-Galán et
144 al., 2013b). Owing to the stratigraphic, structural and petrological styles, the Iberian Massif has
145 been traditionally divided into six tectonostratigraphic zones (Fig. 2; Lozte, 1945; Julivert, 1971):
146 (1) Cantabrian Zone represents a Gondwanan thin-skinned foreland fold-and-thrust belt. It has
147 overall low-grade internal deformation and metamorphism, and represents shortening that
148 occurred during Mississippian times (e.g. Marcos and Pulgar, 1982; Pérez Estaún et al., 1988;
149 Gutiérrez-Alonso 1996; Alonso et al., 2009; Pastor-Galán et al., 2009; 2013b). (2) The West-
150 Asturian Leonese Zone represents a metamorphic fold-and-thrust belt with barrovian
151 metamorphism that collapsed coevally with thrust emplacement onto the Cantabrian Zone (e.g.
152 Martínez-Catalán et al., 1992; Alcock et al., 2009; Martínez-Catalán et al., 2014). (3) The
153 Central Iberian Zone represents the Gondwanan hinterland with Barrovian and Buchan
154 metamorphism and is intruded by igneous rocks of various ages (e.g. Macaya et al., 1991; Díez
155 Balda, 1995; Gutiérrez-Alonso et al., 2018). (4) The Ossa-Morena Zone represents the most
156 distal zone of the Gondwana platform, and is characterized by a metamorphic fold-and-thrust
157 belt with dominantly sinistral displacement (e.g. Robardet and Gutiérrez-Marco, 2004; Quesada,
158 2006). (5) The Galicia-Tras-os-Montes Zone represents a far travelled allochthonous terrane
159 that contains high pressure units and relics of oceanic-like crust (e.g. López-Carmona et al.,
160 2014; Martínez-Catalán et al., 2019). (6) The South Portuguese Zone represents a foreland
161 fold-and-thrust belt with little internal deformation and metamorphism with Avalonian affinity and
162 a strong left-lateral component of shear (e.g. Pereira et al., 2012; Pérez-Cáceres et al., 2016;
163 Oliveira et al., 2019). Geographically, the external zones of the Gondwana margin are nested to
164 the north into the core of the Cantabrian Orocline, whereas the hinterland zones are to the west
165 and center of the massif (Fig. 2; e.g. Díaz Balda, 1995; Azor et al., 2019). The southwestern-
166 most extent of Iberia contains a putative suture of the Rheic ocean, as well as a piece of the



167 Laurussian margin fold-and thrust belt, today preserved in the South Portuguese Zone (e.g.
168 Pereira et al., 2012, 2017; Oliveira et al., 2019).

169 The Gondwanan autochthon stratigraphy (Cantabrian, West Asturian-Leonese, Central
170 Iberian and Ossa Morena Zones) consist of a Neoproterozoic arc and back-arc basin (e.g.
171 Fernández-suárez et al., 2014), which evolved to a rift-to-drift Cambrian to Early Ordovician
172 sequence and then to an Ordovician to Late Devonian passive margin basin sequence (e.g.
173 Sánchez-García et al., 2019; Gutiérrez-Marco et al., 2019; Gutiérrez-Alonso et al., submitted).
174 Overall the system transitioned from a relatively isolated Early Cambrian continental, to a
175 restricted marine basin, to development of an open marine platform that was locally punctuated
176 by magmatism (e.g. Gutiérrez-Alonso et al., 2008b; Palero-Fernández, 2015). The Ossa
177 Morena zone represents the outermost platform, followed by an intermediate platform
178 characterized by an asymmetric horst (Central Iberian Zone) and graben (West-Asturian
179 Leonese Zone), which ends in the innermost shelf environment of the Cantabrian zone (Fig. 3;
180 e.g. Gutiérrez-Marco et al., 2019). The differences between the West Asturian-Leonese and
181 Central Iberian Zone are mainly deeper vs. shallower sedimentary facies (respectively) and a
182 local Lower Ordovician unconformity in the Central Iberian Zone (Toledanian, e.g. Álvaro et al.,
183 2018) that places Lower Ordovician strata atop pre-Cambrian to Cambrian rocks (Fig. 3; e.g.
184 Gutiérrez-Marco et al., 2019). The Central Iberian Zone is divided into two domains: (1) The Ollo
185 de Sapo domain, which contains abundant Lower Ordovician calc-alkaline magmatism (e.g.
186 Díez Montes, 2006; Gutiérrez-Marco et al., 2019); and (2) the ‘Schistose–greywacke Domain’
187 characterized by a predominance of outcrops of Neoproterozoic to Lower Cambrian
188 sedimentary rocks (e.g. Gutiérrez-Marco et al., 2019 and references therein).

189 The Galicia Tras-os-Montes Zone (Farias et al., 1987) is a complex structural stack
190 including a basal schistose unit (Parautochthon; Dias da Silva et al., in press) structurally
191 overlain by mafic rocks with an oceanic-like signature and other far-traveled rocks under high-
192 pressure metamorphism (e.g. López-Carmona et al., 2014; Martínez-Catalán et al., 2019). The
193 oceanic rocks of this zone are classically interpreted as a Rheic Ocean suture (e.g. Martínez
194 Catalán et al., 2009). Recent interpretations support its origin as a minor oceanic basin or
195 seaway within the realm of Gondwana (e.g. Pin et al., 2002; Arenas et al., 2016).

196 The South Portuguese Zone constitutes the Laurussian foreland fold-and-thrust belt in
197 the Iberian Variscides (e.g. Pereira et al., 2012; Pérez-Cáceres et al., 2017). It contains three
198 units: (1) the Pulo de Lobo, a low grade metamorphic accretionary prism with clastic
199 sedimentary rocks and basalts with MORB signature (e.g. Azor et al., 2019; Pérez-Cáceres et
200 al., this volume); (2) The Iberian Pyrite Belt, which is a world class volcanogenic massive sulfide



201 deposit formed between 390 and 330 Ma (e.g. Oliveira et al., 2019a; 2019b); and (3) the Baixo
202 Alentejo Flysch, which is located to the southwest and is a syn-orogenic composite turbiditic
203 sequence with ages from ~330 to ~310 Ma (Oliveira et al., 2019b). The boundary between the
204 South Portuguese and Ossa Morena zones is a sinistral shear zone (so-called Beja-Acebuches,
205 Quesada and Dallmeyer., 1994; Pérez-Cáceres et al., 2016) that contains a strongly deformed
206 amphibolitic belt with oceanic affinity (Munha et al., 1986; Munha, 1989; Quesada et al., 2019).
207 This belt potentially represents dismembered relics of the Rheic ocean and/or a subsidiary
208 seaway that opened during a Variscan transtension event in SW Iberia (e.g. Pérez-Cáceres et
209 al., 2015; Quesada et al., 2019).

210 Finally, Paleozoic rocks occur sporadically within the Alpine Betic chain. Their lithological
211 monotony, paucity of fossils, and the intensity of deformation and metamorphism during Alpine
212 orogeny, make recognizing the original features of the different successions challenging (e.g.
213 Martín-Algarra et al., 2019). Some faunal and detrital zircon studies suggest that the Paleozoic
214 outcrops in the Betics may be similar to the most seaward realms of the Gondwanan platform
215 (i.e., the Cantabrian Zone; e.g. Rodríguez-Cañero et al., 2018; Jabaloy-Sánchez et al., 2018).
216 Following the latest plate reconstructions of the Mediterranean during Meso-Cenozoic times, the
217 Paleozoic units of the Betic-Rif chain may have been located proximal to the present-day
218 position of the Balearic Islands (van Hinsbergen et al., 2020).

219 The Variscan orogen in Iberia shows multiple deformation, metamorphic, and magmatic
220 events (e.g. Martínez-Catalán et al., 2014; Azor et al., 2019; Fig. 2) that evolved diachronously
221 from the suture towards the external zones (Dalmeyer et al., 1997): (1) An initial continent-
222 continent collision began ca. 370-365 Ma, which produced high pressure metamorphism (e.g.
223 Lopez-Carmona et al. 2014). (2) Between 360 and 330 Ma a protracted shortening phase
224 occurred, frequently divided into main phases C1 and C2, that were accompanied by Barrovian
225 type metamorphism (e.g. Dias da Silva et al., in press) and plutonism at ~340 Ma (e.g.
226 Gutiérrez-Alonso et al., 2018). (3) An extensional collapse event, so-called E1, occurred at
227 ~333-317 Ma, which formed core-complexes and granitic domes in the Central Iberian and
228 West Asturian-Leonese zones (Fig. 2C; e.g. Alcock et al., 2009; Díez-Fernández and Pereira,
229 2016; López-Moro et al., 2018). This event is coeval and genetically linked to the formation of
230 the foreland fold-and-thrust-belt of the Cantabrian Zone (e.g. Gutiérrez-Alonso, 1996). (4) A late
231 Carboniferous shortening event (C3) occurred ca. 315-290 Ma and is argued to have resulted in
232 the formation of the Cantabrian Orocline and was accompanied by the intrusion of mantle
233 derived granitoids (Fig. 2C; e.g. Gutiérrez-Alonso et al., 2011a, 2011b; Pastor-Galán et al.,
234 2012a). (5) A final early Permian extensional event (E2), mostly found in the Central Iberian



235 Zone, resulted in the formation of core complexes and regional doming (Dias da Silva et al., in
236 press). (6) A final shortening event (C4), possibly coeval with E2, resulted in widespread brittle
237 deformation (e.g. Azor et al., 2019; Fernández-Lozano et al., 2019).

238 In SW Iberia, the aforementioned Variscan deformation events are characterized by a
239 dominant sinistral component, which contrasts with the general dextral component recognized in
240 most other regions of the orogen (e.g. Martínez Catalán et al., 2011; Gutiérrez-Alonso et al.,
241 2015). Early collisional structures (C1) formed NE-vergent recumbent folds in the southernmost
242 Central Iberian Zone and SW-vergent folds and thrusts in the Ossa Morena and South
243 Portuguese zones. This phase continued with a transtensional event that heterogeneously
244 extended the continental lithosphere (e.g. Pérez-Cáceres et al. 2015). Coevally, an important
245 extension-related magmatic event happened, perhaps assisted by a plume-type mantle
246 (Simancas et al. 2006) or a slab break-off (Pin et al. 2008). After this transtensional event,
247 significant left-lateral transpression occurred forming the extensive shear zones to the north and
248 south of Ossa Morena Zone (Fig. 2B), which accommodated the majority of the transcurrent
249 motion. However, left-lateral displacements are observed all along the Ossa Morena and South
250 Portuguese zones. Pérez-Cáceres et al. (2016) estimated over 1000 km of collisional
251 convergence in SW Iberia, most of which corresponds with left-lateral displacements parallel to
252 terrane boundaries.

253 3 Synthesis on the Geometry and Kinematics of the Cantabrian 254 Orocline

255 Understanding the geometry, kinematic evolution and mechanics of curved mountain
256 systems is crucial to developing paleogeographic and tectonic reconstructions (e.g. Marshak,
257 2004; Van der Voo, 2004; Li et al., 2012; van Hinsbergen et al., 2020). Introduced by Carey
258 (1955 p.257), an orocline (from Greek ορος, mountain, and κλινο, bend) is "...an orogenic
259 system, which has been flexed in plan to a horse-shoe or elbow shape." Although sometimes
260 used in the literature as a geometric description of any orogenic curvature, herein orocline is
261 strictly used as a the term for map-scale bends that underwent vertical-axis rotations (Weil and
262 Sussman, 2004; Johnston et al., 2013; Pastor-Galán et al., 2017a). The kinematic classification
263 of curved mountain belts (Weil and Susman, 2004; Johnston et al, 2013) distinguishes two end
264 members: (1) Primary orogenic curves, which describe those systems in which curvature is a
265 primary feature of the orogen and formed without significant or systematic vertical-axis rotations,
266 and (2) Secondary oroclines, where orogenic curvature was acquired due to vertical-axis
267 rotations subsequent to primary orogenic building. Those systems whose curvature is the



268 product of vertical-axis rotation during the primary orogenic pulse and/or only a portion of the
269 observed curvature is secondary are progressive oroclines.

270 The orocline test (or strike test), evaluates the relationship between changes in regional
271 structural trend (relative to a reference trend for an orogen) and the orientations of a given
272 geologic fabric element or magnetization (relative to a reference direction). In terms of
273 evaluating developmental kinematics, the most relevant geologic marker is paleomagnetic
274 declination, which can be used to quantitatively evaluate total and systematic rotations as a
275 function of along-strike variability. Once acquired, data is plotted on Cartesian coordinate axes
276 with the strike (S) of the orogen (relative to a reference) along the horizontal axis, and the fabric
277 azimuth (F, relative to a reference) along the vertical axis. The test originally used a basic least-
278 squares (OLS) regression (Schwartz and Van der Voo, 1983) to estimate the slope (coded m in
279 formulas), ideally between 0 and 1, which then is interpreted with respect to vertical-axis
280 kinematics. More recently, Yonkee and Weil (2010b) and Pastor-Galán et al. (2017a) introduced
281 more robust statistics to estimate the slope and its uncertainty, considering and propagating
282 errors of the input data. Primary orogenic bends show no change of paleomagnetic declination
283 orientations with varying structural trend, and therefore the slope is expected to be 0. In
284 progressive oroclines, the declination variation records some fraction of the total observed
285 orogenic strike variability, and thus the slope would range between 0 and 1, depending on the
286 amount of primary curvature. Secondary oroclines are those in which the paleomagnetic vectors
287 record 100% of the rotation, yielding slopes of 1, meaning that the orogenic system must have
288 started as a roughly linear system that then underwent secondary vertical-axis rotations until its
289 present-day curvature was acquired. The slope obtained with the orocline test can only be
290 confidently interpreted when the chronology of fabric formation is well known.

291 The trend of the Variscan belt in Iberia follows a sinuous “S” shape that is especially
292 prominent in the northwest region of the Iberian Peninsula, and then becomes more subtle due
293 to the predominance of younger cover sequences in the central and eastern regions of the
294 peninsula (Fig. 1 and 2). This dramatic geometry has stimulated a century long scientific debate
295 as to its origin (e.g. Suess, 1892; Staub, 1926; Martínez Catalán et al., 2015). To the north and
296 convex to the west is the Cantabrian Orocline, and to the center-south and convex to the east is
297 the Central Iberian curve. The overall trend of the Cantabrian Orocline starts in Brittany (France)
298 and southern England and then curves through the Bay of Biscay and then south into central
299 north Iberia (Fig. 1, 2 and 4). The Cantabrian Orocline (also known as Ibero-Armorican Orocline/
300 Arc, Asturian Arc or Cantabrian-Asturias Arc) is arguably the first curved orogen that was
301 scientifically described, recognized by the change in structural trend of mapped thrusts and fold



302 axes (Schultz, 1858, Barrois, 1882, Suess, 1892). The Cantabrian Orocline traces an arc with
303 curvature close to 180° within the central Cantabrian Zone (the Gondwanan foreland in Iberia,
304 fig. 2), and opens to approximately 150° as one moves to the outer arc reaches (Fig. 1). At the
305 crustal-scale, the Cantabrian Orocline represents a first order vertical-axis buckle fold in plan-
306 view that refolds pre-existing Variscan structures (e.g. Julivert and Marcos, 1973; Weil et al.,
307 2001). The inner arc of the orocline, or the Cantabrian Zone is characterized by tectonic
308 transport towards the core of the orocline, i.e., the orocline has a contractional core, where low
309 finite strain values and locally developed cleavage occur (Pérez-Estaún et al., 1988; Gutiérrez-
310 Alonso, 1996; Pastor-Galán et al., 2009). Within the inner core a variety of structures record
311 non-coaxial strain, which produced complex interference folds and rotated thrust sheets (e.g.
312 Julivert and Marcos, 1973; Julivert and Arboleya, 1984; Pérez-Estaún et al., 1988; Aller and
313 Gallastegui, 1995; Weil, 2006, 2013; Pastor-Galán et al., 2012b; Shaw et al., 2015; 2016a; Del
314 Greco et al., 2016). In contrast, the outer arc shows a ca. 150° interlimb angle vertical-axis fold
315 that was accommodated by significant shearing, both dextral and, in lesser amounts, sinistral
316 penecontemporaneous to vertical-axis rotation (Gutiérrez-Alonso et al., 2015). Weil et al. (2013,
317 2019) extensively review the geometry of the Cantabrian Orocline.

318 All kinematic data studied so far support a model in which the Cantabrian Orocline
319 formed due to secondary vertical-axis rotation in a period of time younger than 315 Ma and
320 older than 290 Ma. Overall, the southern limb of the orocline rotated counterclockwise (CCW)
321 and the northern limb clockwise (CW; Fig. 4). Orocline formation happened subsequent to the
322 main shortening phases of the orogen (C1 and C2) and late-stage orogenic collapse (E1), and
323 therefore, it is an ideal example of a secondary orocline in the strictest sense. Development of
324 the Cantabrian Orocline requires the existence of a roughly linear orogenic belt during early
325 Variscan closure of the Rheic Ocean (with a roughly N-S orientation in present-day
326 coordinates), which was subsequently bent in plan-view into an orocline during late stages of
327 Pangea amalgamation. Such interpretation is grounded in paleomagnetic studies (e.g. Hirt et
328 al., 1992; Parés et al. 1994; Stewart, 1995; van de Voo et al., 1997; Weil, 2006; Weil et al.,
329 2000; 2001; 2010), along with important contributions from structural (e.g. Gutiérrez-Alonso
330 1992; Kollmeier et al., 2000; Merino-Tomé et al., 2009; Pastor-Galán et al., 2011; 2014; Shaw et
331 al., 2015) and geochronological studies (e.g., Tohver et al., 2008; Gutiérrez-Alonso et al., 2015).
332 Weil et al. (2013) provides a comprehensive review on the kinematic constraints, updated in
333 2017a by Pastor-Galán et al., and in 2019 by Weil et al.



334 4 The intriguing geometry of the Central Iberian curve

335 The more southern Central Iberian curve has a similar magnitude, but opposite
336 curvature compared to the Cantabrian Orocline (Fig. 1 and 2B). This structure has been referred
337 to as the Central Iberian curve, arc, bend or orocline. In this paper we use 'Central Iberian
338 curve'. The other aforementioned terms involve still unknown parameters or are misleading:
339 orocline imply kinematics (Weil and Sussman, 2004); bend refers to a mechanism of formation
340 (e.g. Fossen, 2016); and arc could be ambiguous, since the term is commonly used for volcanic
341 chains. This curvature was first described by Staub (1926) and was termed the Castilian bend.
342 Continental drift pioneers paid some attention to Staub's description (e.g. Holmes, 1929; Du
343 Toit, 1937), but the curved structure remained largely ignored for multiple decades (e.g.
344 Martínez Catalán et al., 2015). The hypothesis of a large-scale curvature in Central Iberia made
345 a comeback at the beginning of the 21st century with a study of Variscan porphyroblast
346 kinematics across Iberia by Aerden in 2004. Since then, several attempts to unveil its geometry
347 and kinematics have been made with contrasting results.

348 The elusive nature of the Central Iberian curve resides in the poor exposure of its
349 putative hinge (Fig. 2). The hinge of the Cantabrian orocline crops out extensively and the
350 changes in thrust and fold axes trend are observable at high-resolution from aerial photographs
351 and are readily mapped using outcrop-scale observations. In contrast, the alleged hinge of the
352 Central Iberian curve is largely covered by Mesozoic and Cenozoic basins (Fig. 2). The
353 curvature is most recognizable at the boundary between the Galicia-Tras os Montes and Central
354 Iberian zones (Fig. 2A; Aerden, 2004; Martínez Catalán, 2012). The thrust fault that bounds
355 those areas traces close to a 180° of curvature and marks the emplacement of the most distal
356 units. Before the revival of Staub's curved geometry along the entire Central Iberian Zone, there
357 were several attempts to explain the curved shape of the Galicia Tras-os-Montes Zone. Some
358 consider the Galicia Tras-os-Montes Zone a block that escaped during an early Variscan (C1)
359 non-cylindrical collision, forming an extrusion wedge towards the areas undergoing lesser
360 amount of shortening (Martínez-Catalán, 1990, Dias da Silva, 2015; in press); or alternatively a
361 klippe of a larger allochthonous thrust sheet, product of an interference pattern between C2, E1
362 and C3 structures (e.g. Ries and Shackleton, 1971; Martínez Catalán et al., 2002; Rubio
363 Pascual et al., 2013; Díez-Fernández et al., 2015).

364 In addition to the Galicia Tras-os-Montes Zone, other areas showing a certain degree of
365 curvature are to the E and SE of the Central Iberian Zone. There, an approximately 20° change
366 in strike of the Iberian ranges (NE Iberia, Fig. 2A) is observed, which represents the only known
367 outcrop of the hinge of the Central Iberian curve's outer arc. The rest of the curvature has been



368 deduced with indirect observations leading to three competing geometric proposals for the
369 Central Iberia curve (Fig. 2B). The main arguments used to constrain the geometry of the
370 Central Iberian curve are: (1) the geometry of Galicia Tras-os-Montes folds and the orientation
371 of observed garnet inclusion trails (Aerden, 2004; Fig. 2B-1); (2) aligned aeromagnetic
372 anomalies and fold trends in the Iberian ranges and the E-SE Central Iberian Zone (Martínez-
373 Catalán, 2012; Fig. 2A and 2B-2) and; (3) the regional distribution of paleocurrents recorded in
374 Ordovician quartzites (Shaw et al., 2012; Fig. 2B-3 and 3). All proposed geometries share two
375 features: (1) The curvature runs parallel to the Central Iberian Zone, and is located in the
376 center-west of Iberia, and (2) all place the Galicia Tras-os-Montes Zone in the core of the curve
377 with the curves axial trace cross-cutting the Morais Complex, a set of mafic and ultramafic rocks
378 that is roughly circular in shape (Fig. 2B; Dias da Silva et al., in press).

379 Aerden (2004) compared the orientation of inclusions in metamorphic porphyroblasts
380 across the Variscan allochthonous terranes of the NW Iberian Massif, and found that inclusion
381 trails maintain a constant north–south orientation. Comparing such results with the trend of the
382 Variscan fold axes in the central Iberian Zone (Fig. 2A) and a daring interpretation of the
383 aeromagnetic anomalies of the Iberian Peninsula (Fig. 5A), Aerden suggested a geometry in
384 which the Central Iberian curve was more prominent in the outer arc than in the inner arc (Fig.
385 2B-1). In Aerden's view the geometry of the Galicia Tras-os Montes Zone does not represent a
386 large-scale curvature, but rather the original shape of the nappe, perhaps re-tightened during
387 C3 deformation. In contrast, the Iberian Ranges and the SE Central Iberian Zone represent the
388 more curved sector (Fig. 2B-1). In the model of Aerden (2004), the Ossa Morena and South
389 Portuguese Zones are not part of the Central Iberian curvature.

390 Martínez-Catalán (2012) reinterpreted Aerden's analysis of aeromagnetic map data (Fig.
391 5A) and the interpretive structural trends of C1-C2 fold axes from Central Iberian Zone
392 structures (Fig. 2A). In Martínez-Catalán's model, the Central Iberian curvature is a symmetric
393 arcuate shape in which orogen trend changes equally in the inner and outer arc, and is
394 comparable in size to the Cantabrian Orocline, but with opposite curvature and less shortening.
395 This geometric model also excludes the Ossa Morena and the South Portuguese Zones as
396 elements involved in the formation of the curvature (Fig. 2B-2).

397 Finally, Shaw et al. (2012) studied the orientation of paleocurrents in Ordovician
398 Armorican Quartzite (e.g. Aramburu, 2002), which is one of the most prominent rocks exposed
399 in Iberia (Fig. 3). The authors found that paleocurrents fanned outward with respect to the
400 Cantabrian Orocline curve and are approximately perpendicular to the structural trend
401 throughout the peninsula (Fig. 3). Shaw et al. (2012) assumed that the direction and sense of



402 paleocurrents were parallel throughout all zones, and concluded that the Central Iberia curve is
403 a 'S' shape isoclinal structure similar in magnitude to the Cantabrian Orocline (Fig. 2B-3). It is
404 unclear from the Shaw et al. (2012) model the involvement of the Ossa Morena and South
405 Portuguese Zones in the overall curve (if any), nor the prospective location of the external zones
406 of the orogen (Cantabrian Zone) with respect to the overall curvature.

407 5 Move over once, move over twice: Kinematic constraints

408 Late Variscan kinematic data (315-290 Ma; C3, E2, C4 phases) in the Central Iberian
409 curve were scarce prior to revival of Staub's Central Iberian curve (e.g. Vergés, 1983; Julivert et
410 al., 1983; Parés and van der Voo, 1992). More recently, a wealth of studies have been
411 published on the kinematics of forming the Central Iberian curve (Fig. 2B), which are reviewed
412 below.

413 5.1 Structural Geology and Geochronology

414 Curved orogens that result from differential vertical-axis rotations develop remarkable
415 structures within their hinges where compressive and extensive radial structures often develop
416 in combination with tangential shear structures (e.g. Li et al., 2012; Eichelberger and McQuarrie,
417 2015). With the re-emergence of the Central Iberian curve debate, several studies have re-
418 evaluated the well-documented structures from the Central Iberian Zone to constrain the origin
419 and kinematics of curvature. The majority of studies focused on the hinge zone of the curve in
420 the area surrounding Galicia Tras-os-Montes (e.g. Dias da Silva et al., 2014; Jacques et al.,
421 2018a), but some explored more outer-arc areas (e.g. Palero-Fernández et al., 2015; Gutiérrez-
422 Alonso et al., 2015). The following paragraphs synthesize the findings of new field, structural,
423 and geochronological analyses from around the hinge of the Central Iberian curve and its
424 surrounding regions. The reviewed studies identify several deformation events that are linked to
425 regional Variscan deformation phases (Fig. 2A).

426 1. An early generation of upright to overturned cylindrical folds with an associated axial
427 planar cleavage (C1). The C1 fold axes plunge variably from horizontal to nearly vertical
428 (e.g. Jacques et al., 2018a, 2018b). The original trend of the fold axes was parallel to the
429 orogen (e.g. Pastor-Galán et al., 2019b), however interference with younger deformation
430 events has created complicated geometries (e.g. Díez Fernández et al., 2013; Palero-
431 Fernández et al., 2015). The emplacement of the allochthonous units of Galicia Tras-os-
432 Montes zone (commonly referred as C2) is closely associated with development of C1
433 folds, but is restricted to shear zones located along the boundary between the latter and



434 the Central Iberian Zone. This phase includes orogen-parallel emplacement of the
435 allochthonous Galicia Tras-Os Montes units and its associated thrusts (Fig. 2A). The
436 non-coaxial nature of the emplacement of this allochthonous nappe produced folding
437 interference and local vertical-axis rotations (Dias da Silva et al., in press). Prograde
438 Barrovian metamorphism (known as M1) reached its pressure peak at the end of C2
439 (Rubio Pascual et al., 2013).

440 2. After C1 and C2, the resulting thickened crust gravitationally collapsed (Macaya et al.,
441 1991; Escuder Viruete et al., 1994; Díaz-Balda et al., 1995; Díez-Montes, 2010). This
442 gravitational collapse (phase E1) formed gneiss-dome core complexes between 330 and
443 317 Ma (e.g. Díez Fernández and Pereira, 2016) especially at the core of the Central
444 Iberian curve (Fig. 2C; e.g. Martínez-Catalán, 2012). This phase formed large
445 subhorizontal extensional detachments that exhumed to depths of the middle crust (e.g.
446 Rubio-Pascual et al., 2013; Dias da Silva et al., in press). General decompression
447 produced a Buchan-type metamorphic event (M2; e.g. Rubio-Pascual et al., 2016, Solís-
448 Alulima et al., 2019) and widespread anatexis melting (e.g. López-Moro et al., 2018;
449 Pereira et al., 2018). E1 phase developed a fold system with sub-horizontal axes and a
450 penetrative subhorizontal cleavage (e.g. Dias da Silva et al., in press). Mapped folding
451 geometries indicate the deflection of C1 folds into overturned positions within the E1
452 deformation zones (e.g. Díez Fernández et al., 2013; Díez Fernández and Pereira,
453 2016; Pastor-Galán et al., 2019b). In addition to large-scale extensional deformation and
454 Buchan metamorphism, E1 developed a regional dome-and-basin pattern, resulting in
455 portions of the allochthonous terranes tectonically transported into basins (e.g. Días da
456 Silva et al., in press).

457 3. The structures developed during C1-C2 compression and E1 extension, are re-folded by
458 a younger shortening phase (C3; syn-Cantabrian Orocline). C3 formed upright open
459 folds and conjugate sub-vertical shear zones (e.g. Gutiérrez-Alonso et al., 2015; Díez
460 Fernández and Pereira, 2017; Dias da Silva et al., in press). C3 was coeval with regional
461 retrograde metamorphism (M3) and with intrusion of mantle derived granitoids (Fig. 2C;
462 e.g. Gutiérrez-Alonso et al., 2011a), surrounded by contact metamorphic aureoles (e.g.
463 Yenes et al., 1999). The age of the C3 event ranges from 315 and 290 (e.g. Jacques et
464 al., 2018a), concomitant with the formation of the Cantabrian Orocline (e.g. Pastor-Galán
465 et al., 2015a). Ductile deformation, including folding with axial planar cleavage (e.g. Dias
466 da Silva et al., 2014; Pastor-Galán et al., 2019b) and shear zones, occurred at the early
467 stages of C3 (315-305 Ma; Gutiérrez-Alonso et al., 2015; Díez-Fernández and Pereira,



468 2017; Jacques et al., 2018b) followed by brittle deformation that formed cross-joint sets
469 and vein swarms with Sn-W mineralizations (Jacques et al., 2018a; 2018b). The
470 conjugated shear zones, some of them with hundreds of kilometers of displacement, had
471 activity during the period 315-305 based on direct Ar-Ar dating of the shear zones
472 (Gutiérrez-Alonso et al., 2015) and cross-cutting relationships with precisely dated
473 igneous rocks (Díez-Fernández and Pereira, 2017). Note that these shear zones show a
474 younger age with respect to the sinistral shear zones that bound the Ossa Morena and
475 South Portuguese zones (340-330 Ma; e.g. Dallmeyer et al., 1993). New studies in the
476 Central Iberian Zone have determined that several folds, previously interpreted as C1
477 (e.g. the Tamames-Marofa-Sátão synform) are C3 structures, possibly nucleated within
478 existing C1-C2 structures (e.g. Dias da Silva et al., 2017; Jacques et al., 2018b). The
479 remarkable continuity along the Central Iberian Zone of these folds (Fig. 2A), previously
480 interpreted as C1 (e.g. Díez-Balda et al., 1990; Abalos et al., 2002; Dias and Ribeiro,
481 1994; Dias et al., 2016), suggest the ubiquity and importance of this deformation phase.
482 4. Subsequent to C3 deformation, a brittle shortening event (C4) together with some late
483 extensional faults occurred across the region (E2; Fig. 2A; Dias and Ribeiro 1991; Dias
484 et al. 2003; Rubio Pascual et al., 2013; Arango et al., 2013; Fernández-Lozano et al.
485 2019; Dias da Silva et al., in press). E2 developed core complex-like structures that
486 further telescoped the M2 metamorphic isograds between the anatectic cores of gneiss
487 domes and the hanging wall units. This event also favoured sub-horizontal folding and
488 kink-band generation in the upper structural levels. Post-Variscan shortening structures
489 in Northern Iberia are characterized by a N-S compressive regime (C4) allowing the
490 formation of brittle NNE-SSW and NNW-SSE faults and associated sub-vertical and sub-
491 horizontal widespread kink-bands (e.g. Aller et al., 2020).

492 5.2 Paleomagnetism

493 Paleomagnetism investigates the record of the Earth's ancient magnetic field as it is
494 recorded in the rock record. Among other features, rocks can record the orientation of the
495 magnetic field at the time of magnetization (e.g. Tauxe, 2010). The recorded magnetic vector
496 can be geometrically defined by two components: inclination, which is a function of the
497 paleolatitude (being 90° at the poles and 0° at the equator) at the time of magnetization
498 acquisition; and declination, which is a measure of the horizontal angular difference between the
499 recorded magnetic direction and true north, thereby allowing for the quantification of any
500 vertical-axis rotations if a north reference direction is known for the region of interest at the time



501 of magnetization acquisition. Paleomagnetism is the best tool to quantify vertical-axis rotations
502 in orogens due to the independence of the magnetic field from the orogen deformation and
503 evolution (e.g. Butler, 1998).

504 Despite its uniqueness to study paleolatitudes and vertical-axis rotations,
505 paleomagnetism is not flawless. Paleomagnetic data can yield spurious rotations when the local
506 and regional structures are not properly studied and their geometries and kinematic histories not
507 adequately corrected for (e.g. Pueyo et al., 2016). In addition, the age of magnetization
508 acquisition is not necessarily equivalent to the age of the sampled rock. Remagnetizations are
509 ubiquitous, especially in orogens (Weil and van der Voo, 2002; Pueyo et al., 2007; Huang et al.,
510 2017). In remagnetized rocks, the primary magnetization is replaced or overprinted due to a set
511 of geologic processes acting alone or in concert - usually represented by a combination of
512 thermal or chemical reactions (Jackson, 1990). Nevertheless, remagnetizations can be useful
513 for interpreting deformation history if the relative timing of the overprint can be established and a
514 well-constrained reference direction for that age is known (e.g. Weil et al., 2001; Izquierdo-
515 Llavall et al. 2015; Calvin et al., 2017).

516 In addition to knowing the structural geology and the timing of magnetization of the
517 studied rocks, understanding and quantifying local and regional vertical-axis rotations require a
518 paleomagnetic reference pole for comparison. Permian and Mesozoic paleomagnetic studies in
519 Iberia indicate that Iberia was a relatively stable plate from at least Guadalupian times (ca. 270
520 Ma) to the opening of the Bay of Biscay in the Cretaceous (e.g. Gong et al., 2008; Vissers et al.,
521 2016). Weil et al. (2010) calculated the most modern Early Permian pole for stable Iberia, which
522 will be used herein as a reference for any vertical-axis rotation analysis (hereafter, eP pole or
523 eP component). Weil et al.'s Virtual Geomagnetic Pole (VGP) values are $Plat = 43.9$; $Plong =$
524 203.3 and $\alpha_{95} = 5.4$ and when transform into paleomagnetic components has a $\sim 0^\circ$ inclination
525 (equatorial) and declinations that range from 150° to 160° (from NW to SW respectively)
526 depending on where in Iberia you are referencing. In Fig. 6 (red arrows), a compilation of
527 declinations that form part of this composite pole and other eP components found in recent
528 studies are presented.

529 For the Central Iberian curve, the voluminous paleomagnetic database from the
530 Cantabrian Orocline can be used to partially constrain its kinematics (e.g. Weil et al., 2013). The
531 orocline test for the Cantabrian Orocline (fig. 4) quantifies the degree of differential vertical-axis
532 rotation of variously striking Variscan segments in northern Iberia. If the Central Iberian curve is
533 a product of vertical-axis rotation, paleomagnetic declinations would bend around the Central
534 Iberian curve opposite to that of the Cantabrian Orocline. With a well constrained orocline test,



535 as in the Cantabrian Orocline (Fig. 4), one can use the paleomagnetic strike-test correlation
536 slope to establish expected declinations for any along-strike portion of the orogen (Pastor-Galán
537 et al., 2017b).

538 Before the resurgence of the Central Iberian curve, the only available pre-Permian
539 paleomagnetic studies to the South and west of the Cantabrian Zone in the Iberian Massif were
540 focused on the Beja Gabbroic Massif, Portugal (Perroud et al., 1985) and the Almadén syncline
541 volcanics (Perroud et al., 1991; Pares & Van der Voo, 1992). The study in the Beja area showed
542 varied inclinations and declinations in the gabbros, and complex overprints elsewhere. Perroud
543 et al (1985) did not consider any structural correction for the results, assuming the gabbro was
544 undeformed. Recently, Dias da Silva et al. (2018) showed that the area underwent intense
545 deformation during the Carboniferous. Therefore interpretation of this dataset is complicated
546 without knowing the proper structural correction needed to restore the magnetization to its
547 palinspastic orientation.

548 Several articles with new paleomagnetic studies around the Central Iberian curve have
549 been published since 2015 (Fig. 5). In general, these studies have reported a pervasive late
550 Carboniferous (320 to 300 Ma) (re-)magnetization in sedimentary and igneous rocks (e.g.
551 Pastor-Galán et al., 2015a; 2017b; Fernández-Lozano et al. 2016), which is largely
552 penecontemporaneous to the intrusion of E1 extensional granites (López-Moro et al., 2018) and
553 C3 syn-orocline mantle derived granitoids (Fig. 2C; e.g. Gutiérrez-Alonso et al., 2011a). The
554 following section describes the magnetizations from oldest to youngest.

555 Pastor-Galán et al. (2016) sampled for paleomagnetic analyses both E1 extensional
556 granites (Fig. 2C; ~320 Ma; e.g. López-Moro et al., 2018) from the Tormes and Martinamor
557 domes, and C3 mantle derived granitoids in the Central System (Fig. 2C; 305-295 Ma; e.g.
558 Gutiérrez-Alonso et al., 2011a). Both sets of plutons are located around the Galicia Tras-os-
559 Montes hinge of the Central Iberian curve (Fig. 6-5). The authors found an original component in
560 E1 granites supported by a positive reversal test in both domes (Fig. 7). The magnetization has
561 an inclination (Inc.) = 15° (paleolatitude (λ) = -7.6°) and declination (Dec.) = 81° (Fig. 7), which
562 imply a northward movement of 700 km and a ~70° CCW rotation with respect to the C3
563 granites that showed an eP component (Dec. ~ 150, Inc. ~ 0). Considering the positive reversal
564 test in E1 granites and the significant difference in inclinations with respect to C3 granitoids (eP
565 component), a magnetization age of older than 318 Ma was proposed (pre Kiaman superchron,
566 317 Ma - 267 Ma, e.g. Langereis et al., 2010), which was interpreted as a primary
567 magnetization. The 70° CCW Pennsylvanian rotation recorded in rocks from the Central Iberian
568 curve hinge zone is in agreement with the expected rotation of the southern limb of the



569 Cantabrian Orocline (Fig. 4; Weil et al., 2013).

570 At the putative outer arc of the Central Iberian curve, the Iberian Ranges (Fig. 2),
571 paleomagnetic and structural studies of Devonian and Permian rocks (Pastor-Galán et al.,
572 2018) revealed that the eP component from Permian rocks had rotated $\sim 22^\circ$ CW during the
573 Cenozoic (Fig. 8; cf. Pastor-Galán et al., 2018). The Permian and Mesozoic rocks from the
574 Iberian Ranges show a consistent $\sim 22^\circ$ CW rotation with respect to the Apparent Polar Wander
575 Path for Iberia (e.g. Pastor-Galán et al. 2018). This rotation likely happened during the Alpine
576 orogeny, in which the northern area of the Iberian Range underwent more shortening than the
577 southern part, resulting in a regional CW vertical-axis rotation (Izquierdo-Llavall et al., 2019).
578 After restoring the Cenozoic rotation, the Devonian rocks show a positive reversal and fold-test
579 with inclinations that are steeper than expected from the eP component (Dec. = 85.3° , Inc. =
580 12.7° , $\lambda = -6.4$). This component is statistically indistinguishable from that of the E1 granites and
581 the southern branch of the Cantabrian Zone, showing the same 70° CCW rotation from the time
582 they were remagnetized (estimated in 318 Ma) to the timing of the eP component (Fig. 8;
583 Pastor-Galán et al., 2018). Once Cenozoic rotation is corrected for, the structural and
584 paleomagnetic trends of the Iberian ranges become parallel to those in the southern limb of the
585 Cantabrian Orocline, ruling out a Variscan or older origin for the outer Central Iberian curve (Fig.
586 8).

587 The remaining paleomagnetic works published on Central and SW Iberia rocks all reveal
588 a ubiquitous late Carboniferous to Early Permian remagnetizations during the Kiaman
589 superchron (Fernández-Lozano et al., 2016; Pastor-Galán et al., 2015a; 2016; 2017b; Leite
590 Mendes, in press). The authors of these papers calculated the expected declination for each
591 site as if they were part of the Cantabrian Orocline (Fig. 9A). All localities where magnetizations
592 pre-date the formation of the Cantabrian Orocline show the same expected rotations as the
593 southern limb of the Cantabrian Orocline, regardless of their position within the Central Iberian
594 curve (to the hinge: Tormes and Martinamor domes, Iberian ranges; to the southern limb:
595 Almadén syncline and South Portuguese Zone). Other locations, especially limestones from the
596 Central Iberian Zone, have declinations and inclinations in between the primary 318 Ma
597 component of the E1 granites and the post-orocline eP component (Fig. 9B). Pastor-Galán et al.
598 (2015a; 2016) interpreted these results as being caused by a remagnetization that was acquired
599 during Cantabrian Orocline formation and therefore recorded intermediate steps between the
600 component of the E1 granites and eP. Those authors suggest that the large amount of syn-
601 orocline mantle derived granitoids that intruded the Central Iberian Zone (C3 granitoids)
602 triggered the hinterland remagnetization.



603 Finally, two previous studies identified an earlier magnetization in the Almadén syncline
604 region of the SE Central Iberian Zone (Perroud et al., 1991; Pares & Van der Voo, 1992).
605 However, Leite Mendes et al. (in press) argue that these studies are likely misinterpreted.
606 Perroud et al. (1991), applied a complicated structural correction restoring a putative plunge of
607 the regional structural axis to all sites, including those where the syncline axis does not plunge.
608 Leite Mendes et al. (in press) re-sampled the syncline where its axis is sub-horizontal and
609 obtained a negative fold test, implying that the magnetization is not primary as previously
610 interpreted. Their results, however, are similar in orientation to those components published
611 from previous studies prior to any structural correction (Perroud et al., 1991 and Parés and van
612 der Voo, 1992).

613 Two additional studies sampled Laurussian margin sequences that are today adjacent to
614 the Cantabrian Orocline region (Fig. 10). To the north, the SW area of Ireland preserves a Late
615 Paleozoic basin filled with Devonian red sandstone and Carboniferous limestone and siltstone,
616 which was sampled by Pastor-Galán et al. (2015a). To the south is the aforementioned results
617 from the South Portuguese Zone (Leite Mendes et al., in press). Both areas are interpreted to
618 have previously been part of the Laurussian continent, on the opposite side of the Rheic Ocean
619 suture at the time of Variscan collision (Fig. 10; e.g. Pastor-Galán et al., 2015b). In contrast, the
620 rest of Iberia was part of, or proximal to, Gondwana (e.g. Franke et al., 2017). These
621 Paleomagnetic results from the Laurussian margin suggest that the rotations involved in the
622 formation of the Cantabrian Orocline occurred along both sides of the Rheic suture proximal to
623 both its northern and southern limb (Fig. 10A and B). Pastor-Galán et al. (2015b) hypothesized
624 a so-called Greater Cantabrian Orocline that would have bent the entire Appalachian/Variscan
625 orogen around a vertical-axis, affecting at least the continental margins of both Gondwana and
626 Laurussia.

627 5.3 The implications of not being a secondary orocline

628 The most relevant new data regarding the kinematics of the Central Iberian curve is the
629 paleomagnetic study from the Iberian Ranges (Calvín et al., 2014; Pastor-Galán et al., 2018).
630 These results confirm that the present-day variation in trend of the tectonostratigraphic units,
631 generally attributed to Variscan tectonics (e.g. Weil et al., 2013; Shaw et al., 2012; 2014), is
632 likely a product of Cenozoic Alpine orogeny. Izquierdo-Llavall et al. (2019) confirmed that the
633 interpreted Alpine rotations correspond well with the amount of shortening reconstructed in
634 Meso-Cenozoic basins. The best preserved and most continuous outcrop in the Central
635 Iberian's outer arc is not a Variscan structure, casting doubt that Central Iberian curve's is



636 related to Variscan kinematics. The results are also a reminder that the regional effects of
637 Alpine deformation are often underestimated, especially close to the major Iberian Alpine fronts:
638 the Pyrenees, Iberian Ranges, and the Betics.

639 Overall, new paleomagnetic data from the Central Iberian curve and nearby areas reveal
640 pervasive late Carboniferous remagnetizations and regional vertical-axis rotations of the same
641 sense and magnitude to those expected for the southern arm of the Cantabrian Orocline. The
642 new paleomagnetic data indicate that a post ~320 Ma formation for the Central Iberia curve due
643 to vertical-axis rotations is not supported (Pastor-Galán et al., 2016). The distribution in space
644 and time of paleomagnetic results discards the formation of the Central Iberian curve as a
645 product of Variscan gravitational collapse (E1, ~330-317 Ma) or concomitant to the Cantabrian
646 Orocline (C3). So far, no pre-E2 paleomagnetic component has been found, and consequently,
647 paleomagnetic data cannot reject an early orogenic origin for the inner arc of the Central Iberian
648 curve (C1-C2, older than 330 Ma).

649 From a structural geology point of view, the Central Iberian curve does not display the
650 classic geometries and structural interference patterns as found in other established oroclines
651 (i.e., those systems that involve differential vertical-axis rotations, e.g. Li et al., 2012; van der
652 Boon et al., 2018; Meijers et al., 2017; Rezaeian et al., in press). The geometry and structural
653 behaviour of oroclines should resemble, at the crustal-scale, a regional vertical-axis fold
654 preserved in plan-view, either formed by buckling (e.g. Johnston et al., 2001) or bending (e.g.
655 Cifelli et al., 2008) mechanisms. In oroclines, pre-existing structures tend to follow fold trends
656 around the curvature (e.g. Rosenbaum, 2014; Li et al., 2018). In addition, orocline cores tend to
657 preserve radial structures and shortening patterns in the inner arc and orocline parallel shear
658 zones and extension structures in their outer arc (e.g. Ries and Shackleton, 1976; Eichelberger
659 and McQuarrie, 2015), similar to what is observed in multilayer folds (e.g. Fossen, 2016).

660 The structural geometry of the Central Iberian curve lacks such patterns.
661 Paleomagnetism from the Iberian Ranges indicate that the Cantabrian and West Asturian
662 Leonese zones do not follow the Central Iberian curve, instead they continue their NWW-SEE
663 trend into the Mediterranean in what it is now the Betic chain (Rodríguez-Cañero et al., 2018;
664 Jabaloy-Sánchez et al., 2018; van Hinsbergen et al., 2020). Structural trends in the Ossa
665 Morena and the South Portuguese Zone do not show any change in along-strike structural trend
666 that supports large-scale CW rotations (e.g. Pérez-Cáceres et al., 2015; Quesada et al., 2019),
667 whereas existing paleomagnetic data from those zones (Leite Mendes et al., in press) support a
668 model of CCW rotation associated with the broader southern arm of the Cantabrian Orocline. In
669 the Central Iberian and Galicia Tras-os-Montes zones, the trend of curvature is irregular (see C1



670 fold patterns in Fig. 2A) and nowhere are the expected inner and outer arc-related structures
671 preserved (e.g. Dias da Silva et al. in press).

672 The curved shape of C1 fold axes in the Central Iberian zone is better explained by fold
673 interference patterns than vertical-axis rotations (e.g. Pastor-Galán et al., 2019b). Moreover, the
674 curved shape of the Galicia Tras-os-Montes allochthonous nappe, which was emplaced orogen
675 parallel, shows no evidence of vertical-axis rotation related structures (Fig. 2A; Dias da Silva et
676 al., in press). Other authors describe the changes in trend around the Central Iberian curve
677 expressed by C1 folds (Fig. 2A) as the product of fold interference patterns (e.g. Gutiérrez-
678 Alonso, 2009; Palero-Fernández et al., 2015; Jacques et al., 2018b; Dias da Silva et al., in
679 press). Pastor-Galán et al. (2019b) showed that curved C1 folds in the Central Iberian Zone
680 around the Galicia Tras-os-Montes boundary (Fig. 2A) are coaxial with C3 folds after restoring
681 the effects of C2 and E1 deformation phases (Fig. 11A). Both C1 and C3 formed under similar
682 shortening directions. In the same area, Jacques et al. (2018b) found similar fold interference
683 patterns, in addition they described kinematic incompatibility with the expected CW rotations
684 that would have occurred if the Central Iberian curve was an orocline. In other areas of the
685 Central Iberian Zone, the curved shape of C1 folds has been described as an interference
686 between C1 structures and their reorientation caused by C3 shear zones (Fig. 2A; e.g. Palero-
687 Fernández et al., 2015; Dias et al., 2016), or alternatively the interference between C1, C3 and
688 the E2 structures (Fig. 2A; Gutiérrez-Alonso, 2009; Arango et al., 2013; Rubio Pascual et al.
689 2013).

690 Overall, new geometric and kinematic data favor the interpretation that the Central
691 Iberian curve is not a structure formed by differential vertical-axis rotation as was the Cantabrian
692 Orocline, but one formed as a consequence of several competing processes. It is clear from the
693 current data that a combination of several deformation events caused the orientation of
694 structures that today delineate the shape of the Central Iberia curve. These include: (1) the
695 northern part of the outer-arc is the product of an Alpine rigid block rotation instead of Variscan
696 differential vertical-axis rotation (Pastor-Galán et al., 2018); (2) the curvature of the Galicia Tras-
697 os-Montes allochthonous nappe reflects its original shape and could be defined as a primary
698 curve (see Weil and Sussman, 2004), since it was emplaced orogen parallel and shows no sign
699 of vertical-axis rotations at any time (fig. 2A; Dias da Silva et al., in press); (3) Structural
700 analysis shows that fold interference patterns explain the geometry of the curved trends of
701 Central Iberian Zone's C1 folds (Pastor-Galán et al., 2019b), whose kinematics are incompatible
702 with the required CW rotations expected if the curve is an orocline (Jacques et al, 2018b).



703 6 Get Back: Ideas flowing out and endless questions

704 The pioneering works in the last decade that resurrected the idea of a Central Iberian
705 curve, speculated that both the Cantabrian and Central Iberian zones buckled together as
706 secondary oroclines (Fig. 12; Martínez-Catalán 2011; Shaw et al., 2012, 2014; Shaw and
707 Johnston, 2016; Carreras and Druguet, 2014). Later, Martínez Catalan et al. (2014) and Díez
708 Fernández and Pereira (2017) reformulated Martínez-Catalán's 2011 hypothesis and proposed
709 that the Central Iberian curve formed as an orocline between 315 and 305 Ma, and assigning
710 the Cantabrian Orocline a time frame between 305 and 295 Ma (Fig. 12). The proposed tectonic
711 mechanisms to support these early kinematic models are varied: (1) buckling of a ribbon
712 'Armorican' continent (Fig. 12A; Shaw et al., 2014; 2016); (2) buckling of a completely formed
713 Variscan orogen during a putative 'Pangea B' to 'Pangea A' transition in the late Carboniferous
714 (Fig. 12B; Carreras and Druguet, 2014; Martínez-Catalán et al., 2011); (3) indentation of
715 Laurussia into Gondwana during the early stages of collision (at present day SW Iberia, South
716 Portuguese Zone), producing first the Central Iberian curve as a mega drag-fold during
717 Carboniferous times and then slightly later the Cantabrian Orocline as a consequence of an
718 indentation process (fig. 12C; Simancas et al., 2013).

719 The reviewed data in sections 4 and 5 contradict the aforementioned hypotheses.
720 Paleomagnetism and structural patterns (section 5; Fig. 6-11) disagree with the necessary CW
721 rotations required to support a late Carboniferous orocline origin for the Central Iberian curve
722 (Models in Fig. 12A and B). In addition, the sense and magnitude of the vertical-axis rotations
723 observed in SW Iberia (Fig. 10) imply that the South Portuguese (Avalonian segment) and Ossa
724 Morena zones moved together with the southern limb of the Cantabrian Orocline during the
725 Pennsylvanian and Early Permian. This means that the South Portuguese Zone was already
726 parallel to the general trend of the Variscan orogen prior to Cantabrian Orocline formation,
727 implying the lack of a Laurussian rigid indenter into Gondwana (e.g. Simancas et al., 2013). This
728 discrepancy leaves orogen-parallel terrane transport as a possible explanation to the kinematics
729 observed in Ossa Morena and South-Portuguese Zones (e.g. Pérez-Cáceres et al., 2016). At
730 the same time, paleomagnetism from SW Iberia backs the hypothesis of a Greater Cantabrian
731 Orocline extended into both Gondwana and Laurussia in its northern and southern limbs (Fig.
732 10; Pastor-Galán et al., 2015b).

733 In spite of the kinematic constraints and structural patterns, which do not support a
734 vertical-axis origin for the Central Iberian curve in Late Carboniferous time, other geometric
735 constraints remain challenging. The curved shape of the aeromagnetic and gravity anomalies of
736 Iberia are real (Fig. 5). These striking patterns could be due to Variscan-Alpine structural



737 interference, for example the previous example from the Iberian Ranges, but currently there is
738 not enough data to rigorously test this hypothesis. Shaw et al. (2012) supported their hypothesis
739 of a secondary orocline by assuming that paleocurrents were parallel through Iberia during
740 Ordovician times. However, some of the observed deflections in the paleocurrents studied by
741 Shaw et al. (2012; see Fig. 3) are also explained by Alpine vertical-axis rotations (the case of
742 the Iberian ranges) and fold interference patterns (SE of the Central Iberian Zone). Others
743 (Central and SW of the Central Iberian Zone) may be explained by a local response to basin
744 architecture (Fig. 3), where paleo-flow directions would trend toward the deepest basin
745 throughs. The Ordovician basin architecture of Iberia allows for opposite directed paleocurrents
746 from both sides of such throughs (Fig. 3). However, the Early Paleozoic basin architecture in
747 Iberia and their local deformation events require further research (Sánchez-García et al., 2019).

748 Although kinematic evidence is still scarce for the earliest Variscan movements, we
749 argue that pre-orogenic physiographic features, such as the opening of a marginal restricted
750 ocean between Gondwana and its distal platform at 395 Ma (Fig. 13A; Pin et al., 2002;
751 Gutiérrez-Alonso et al., 2008b; Arenas et al., 2016) explains the rounded shape of the Galicia
752 tras-os-Montes curve as a primary arc. During the collision, the latter irregularity would cause
753 the orogen-parallel emplacement of allochthonous nappe (Fig. 13B; Dias da Silva et al., in
754 press) and the left-lateral movements of the Ossa Morena and South Portuguese Zones in SW
755 Iberia (Fig 13A, B, C; Quesada, 2019). During the late Carboniferous, possibly due to a plate
756 reorganization during the final amalgamation of Pangea (Fig. 13D; e.g. Gutiérrez-Alonso et al.,
757 2008a; Pastor-Galán et al., 2015a), the far-field stress-field likely changed and buckled the
758 entire orogen around a vertical axis (Gutiérrez-Alonso et al., 2004), including both the
759 Gondwana and Laurussia margins (Fig. 13E; Pastor-Galán et al., 2015b).

760 Acknowledgements

761 DPG thanks the extraordinary hard work, patience and endurance of the Utrecht
762 University students that embraced and enjoyed studying the kinematics of the central Iberian
763 curvature: Thomas Groenewegen, Bart Ursem, Daniel Brower, Mark Diederer and Bruno Leite-
764 Mendes. DPG acknowledges FRIS and CNEAS for the continuous financial support. GGA is
765 supported by Spanish Ministry of Science, innovation and universities under the project
766 IBERCRUST (PGC2018-096534-B-I00) and Russian Federation Government grant no.
767 14.Y26.31.0012. This paper is a contribution to the IGCP no. 648 “Supercontinent Cycles and
768 Global Geodynamics”. 50 years ago four fabulous guys let it be and never got back.



769 References

- 770 Ábalos, B., Carreras, J., Druguet, E., Escuder Viruete, J., Gómez Pugnare, M. T., Lorenzo
771 Álvarez, S., Quesada, C., Rodríguez Fernández, L. R. and Gil-Ibarguchi, J. I.: Variscan and pre-
772 Variscan tectonics, *Geol. Spain*, 155–183, 2002.
- 773 Aerden, D.: Correlating deformation in Variscan NW-Iberia using porphyroblasts; implications for
774 the Ibero-Armorican Arc, *J. Struct. Geol.*, 26(1), 177–196, 2004.
- 775 Alcock, J. E., Catalán, J. R. M., Arenas, R. and Montes, A. D.: Use of thermal modeling to
776 assess the tectono-metamorphic history of the Lugo and Sanabria gneiss domes, Northwest
777 Iberia, *Bull. Société Géologique Fr.*, 180(3), 179–197, doi:10.2113/gssgfbull.180.3.179, 2009.
- 778 Aller, J., Bastida, F. and Bobillo-Ares, N. C.: On the development of kink-bands: A case study in
779 the West Asturian-Leonese Zone (Variscan belt, NW Spain) / Sur le développement des kink-
780 bands : un exemple dans le Zone Astur Occidentale-Léonaise (chaîne varisque ibérique, nord-
781 ouest de l'Espagne), *Bull. Société Géologique Fr.*, 191(1), doi:10.1051/bsgf/2020003, 2020.
- 782 Aller, J. J. J. and Gallastegui, J. J.: Analysis of kilometric-scale superposed folding in the
783 Central Coal Basin (Cantabrian zone, NW Spain), *J. Struct. Geol.*, 17(7), 961–969,
784 doi:10.1016/0191-8141(94)00115-G, 1995.
- 785 Alonso, J. L., Marcos, A. and Suárez, A.: Paleogeographic inversion resulting from large out of
786 sequence breaching thrusts: The León Fault (Cantabrian zone, NW Iberia). A new picture of the
787 external Variscan thrust belt in the Ibero-Armorican arc, *Geol. Acta*, 7(4), 451–473,
788 doi:10.1344/105.000001449, 2009.
- 789 Álvaro, J. J., Casas, J. M., Clausen, S. and Quesada, C.: Early Palaeozoic geodynamics in NW
790 Gondwana, *J. Iber. Geol.*, 44(4), 551–565, doi:10.1007/s41513-018-0079-x, 2018.
- 791 Ardizzone, Juan, Julio Mezcuca, and Isabel Socías. Mapa aeromagnético de España peninsular.
792 Instituto Geográfico Nacional, 1989.
- 793 Mergl, M. & Zamora, S. 2012, New and revised occurrences of... *Bulletin of Geosciences*, 87,
794 571–586., [online] Available from: <http://www.geology.cz/bulletin/contents/art1327> (Accessed 6
795 April 2020b), n.d.
- 796 Aramburu, C., Méndez-Bedia, I. and Arbizu, M.: The Lower Palaeozoic in the Cantabrian Zone
797 (Cantabrian Mountains, NW Spain), edited by S. García-López and F. Bastida, pp. 35–49.,
798 2002.
- 799 Arango, C., Díez Fernández, R. and Arenas, R.: Large-scale flat-lying isoclinal folding in
800 extending lithosphere: Santa María de la Alameda dome (Central Iberian Massif, Spain),
801 *Lithosphere*, 5(5), 483–500, doi:10.1130/L270.1, 2013.
- 802 Arenas, R., Sánchez Martínez, S., Díez Fernández, R., Gerdes, A., Abati, J., Fernández-
803 Suárez, J., Andonaegui, P., González Cuadra, P., López Carmona, A., Albert, R., Fuenlabrada,
804 J. M. and Rubio Pascual, F. J.: Allochthonous terranes involved in the Variscan suture of NW
805 Iberia: A review of their origin and tectonothermal evolution, *Earth-Sci. Rev.*, 161, 140–178,
806 doi:10.1016/j.earscirev.2016.08.010, 2016.



- 807 Ayala, C., Bohoyo, F., Maestro, A., Reguera, M. I., Torne, M., Rubio, F., Fernández, M. and
808 García-Lobón, J. L.: Updated Bouguer anomalies of the Iberian Peninsula: a new perspective to
809 interpret the regional geology, *J. Maps*, 12(5), 1089–1092,
810 doi:10.1080/17445647.2015.1126538, 2016.
- 811 Ayarza, P., Catalan, J. R. M., Gallart, J., Pulgar, J. A. and Danobeitia, J. J.: Estudio Sismico de
812 la Corteza Iberica Norte 3.3: A seismic image of the Variscan crust in the hinterland of the NW
813 Iberian Massif, *Tectonics*, 17(2), 171–+, 1998.
- 814 Azor, A., Rubatto, D., Simancas, J. F., Lodeiro, F. G., Poyatos, D. M., Parra, L. M. M. and
815 Matas, J.: Rhenic Ocean ophiolitic remnants in Southern Iberia questioned by SHRIMP U-Pb
816 zircon ages on the Beja-Acebuches amphibolites - art. no. TC5006, *Tectonics*, 27(5), C5006–
817 C5006, 2008.
- 818 Azor, A., Dias da Silva, Í., Gómez Barreiro, J., González-Clavijo, E., Martínez Catalán, J. R.,
819 Simancas, J. F., Martínez Poyatos, D., Pérez-Cáceres, I., González Lodeiro, F., Expósito, I.,
820 Casas, J. M., Clariana, P., García-Sansegundo, J. and Margalef, A.: Deformation and Structure,
821 in *The Geology of Iberia: A Geodynamic Approach*, edited by C. Quesada and J. T. Oliveira, pp.
822 307–348, Springer International Publishing, Cham., 2019.
- 823 Barrois, C. E.: Recherches sur le terrains anciens des Asturies et de la Galice, Six-Horemans.,
824 1882.
- 825 Bastida, F.: Zona Cantábrica, in *Geología de España*, edited by J. A. Vera, pp. 25–49, SGE-
826 IGME, Madrid., 2004.
- 827 Bayona, G., Thomas, W. A. and Van der Voo, R.: Kinematics of thrust sheets within transverse
828 zones: A structural and paleomagnetic investigation in the Appalachian thrust belt of Georgia
829 and Alabama, *J. Struct. Geol.*, 25(8), 1193–1212, doi:10.1016/S0191-8141(02)00162-1, 2003.
- 830 van der Boon, A., van Hinsbergen, D. J. J. J., Rezaeian, M., Gürer, D., Honarmand, M.,
831 Pastor-Galán, D., Krijgsman, W. and Langereis, C. G. G.: Quantifying Arabia–Eurasia
832 convergence accommodated in the Greater Caucasus by paleomagnetic reconstruction, *Earth
833 Planet. Sci. Lett.*, 482, doi:10.1016/j.epsl.2017.11.025, 2018.
- 834 Buitter, S. J. H. and Torsvik, T. H.: A review of Wilson Cycle plate margins: A role for mantle
835 plumes in continental break-up along sutures?, *Gondwana Res.*, 26(2), 627–653,
836 doi:10.1016/j.gr.2014.02.007, 2014.
- 837 Butler, R.: Paleomagnetism: Magnetic domains to geologic terranes, *Electron. Ed.*,
838 (September), 319–319, doi:10.1006/icar.2001.6754, 1998.
- 839 Calvin, P., Casas, A. M., Villalaín, J. J., Tierz, P., Calvin, P., Casas, A. M., Villalaín, J. J., Tierz,
840 P., Calvin, P., Casas, A. M., Villalaín, J. J. and Tierz, P.: Reverse magnetic anomaly controlled
841 by Permian Igneous rocks in the Iberian Chain (N Spain), *Geol. Acta*, 12(3), 193–207,
842 doi:10.1344/GeologicaActa2014.12.3.2, 2014.
- 843 Calvin, P., Casas-Sainz, A. M. M., Villalaín, J. J. J. and Moussaid, B.: Diachronous folding and
844 cleavage in an intraplate setting (Central High Atlas, Morocco) determined through the study of
845 remagnetizations, *J. Struct. Geol.*, 97, 144–160, doi:10.1016/j.jsg.2017.02.009, 2017.



- 846 Calvín-Ballester, P. and Casas, A.: Folded Variscan thrusts in the Herrera Unit of the Iberian
847 Range (NE Spain), *Geol. Soc. Lond. Spec. Publ.*, 394(1), 39–52, doi:10.1144/SP394.3, 2014.
- 848 Carey, S. W.: The orocline concept in geotectonics-Part I, *Pap. Proc. R. Soc. Tasman.*, 89,
849 255–288, 1955.
- 850 Carreras, J. and Druguet, E.: Framing the tectonic regime of the NE Iberian Variscan segment,
851 *Geol. Soc. Lond. Spec. Publ.*, 405(1), 249–264, doi:10.1144/SP405.7, 2014.
- 852 Martínez-Catalán, J. R. M., Fernández-Suárez, J., Jenner, G. A., Belousova, E. and Montes, A.:
853 Provenance constraints from detrital zircon U–Pb ages in the NW Iberian Massif: implications
854 for Palaeozoic plate configuration and Variscan evolution, *J. Geol. Soc.*, 161(3), 463–476,
855 doi:10.1144/0016-764903-054, 2004.
- 856 Chopin, F., Schulmann, K., Skrzypek, E., Lehmann, J., Dujardin, J. R., Martelat, J. E., Lexa, O.,
857 Corsini, M., Edel, J. B., Štípská, P. and Pitra, P.: Crustal influx, indentation, ductile thinning and
858 gravity redistribution in a continental wedge: Building a Moldanubian mantled gneiss dome with
859 underthrust Saxothuringian material (European Variscan belt), *Tectonics*, 31(1), n/a-n/a,
860 doi:10.1029/2011TC002951, 2012.
- 861 Chopin, F., Corsini, M., Schulmann, K., El Houicha, M., Ghienne, J.-F. and Edel, J.-B.: Tectonic
862 evolution of the Rehamna metamorphic dome (Morocco) in the context of the Alleghanian-
863 Variscan orogeny, *Tectonics*, 33(6), 1154–1177, doi:10.1002/2014TC003539, 2014.
- 864 Cifelli, F., Mattei, M. and Della Seta, M.: Calabrian Arc oroclinal bending: The role of subduction,
865 *Tectonics*, 27(5), doi:10.1029/2008TC002272, 2008.
- 866 Dallmeyer, R. D., Fonseca, P. E., Quesada, C. and Ribeiro, A.: 40Ar/39Ar mineral age
867 constraints for the tectonothermal evolution of a Variscan suture in southwest Iberia,
868 *Tectonophysics*, 222(2), 177–194, doi:10.1016/0040-1951(93)90048-O, 1993.
- 869 Dallmeyer, R. D. D., Catalán, J. R. M., Arenas, R., Gil Iburguchi, J. I. I., Gutiérrez-Alonso, G.,
870 Farias, P., Bastida, F. and Aller, J.: Diachronous Variscan tectonothermal activity in the NW
871 Iberian Massif: Evidence from 40Ar/39Ar dating of regional fabrics, *Tectonophysics*, 277(4),
872 307–337, doi:10.1016/S0040-1951(97)00035-8, 1997.
- 873 Dias da Silva, Í., Gómez-Barreiro, J., Martínez Catalán, J. R., Ayarza, P., Pohl, J. and Martínez,
874 E.: Structural and microstructural analysis of the Retortillo Syncline (Variscan belt, Central
875 Iberia). Implications for the Central Iberian Orocline, *Tectonophysics*, 717, 99–115,
876 doi:10.1016/j.tecto.2017.07.015, 2017.
- 877 Dias da Silva, Í., Pereira, M. F., Silva, J. B. and Gama, C.: Time-space distribution of silicic
878 plutonism in a gneiss dome of the Iberian Variscan Belt: The Évora Massif (Ossa-Morena Zone,
879 Portugal), *Tectonophysics*, 747–748, 298–317, doi:10.1016/j.tecto.2018.10.015, 2018.
- 880 Dias da Silva, Í., González Clavijo, E. and Díez-Montes, A.: The collapse of the Variscan belt: a
881 Variscan lateral extrusion thin-skinned structure in NW Iberia, *Int. Geol. Rev.*, 00(00), 1–37,
882 doi:10.1080/00206814.2020.1719544, in press.
- 883 Dias da Silva, Í. F., Linnemann, U., Hofmann, M., González-Clavijo, E., Díez-Montes, A. and
884 Catalán, J. R. M.: Detrital zircon and tectonostratigraphy of the Parautochthon under the Morais



- 885 Complex (NE Portugal): implications for the Variscan accretionary history of the Iberian Massif,
886 *J. Geol. Soc.*, 172(1), 45–61, doi:10.1144/jgs2014-005, 2015.
- 887 Dias, R. and Ribeiro, A.: Finite strain analysis in a transpressive regime (Variscan autochthon,
888 northeast Portugal), *Tectonophysics*, 191(3), 389–397, doi:10.1016/0040-1951(91)90069-5,
889 1991.
- 890 Dias, R. and Ribeiro, A.: CONSTRICTION IN A TRANSPRESSIVE REGIME - AN EXAMPLE IN
891 THE IBERIAN BRANCH OF THE IBERO-ARMORICAN ARC, *J. Struct. Geol.*, 16(11), 1543–
892 1554, 1994.
- 893 Dias, R., Ribeiro, A., Romão, J., Coke, C. and Moreira, N.: A review of the arcuate structures in
894 the Iberian Variscides; constraints and genetic models, *Tectonophysics*, 681, 170–194,
895 doi:10.1016/j.tecto.2016.04.011, 2016.
- 896 Díez Balda, M. A., Vegas, R. and González Lodeiro, F.: Central-Iberian zone structure, Pre-
897 Mesoz. Geol. Iber., 172–188, 1990.
- 898 Díez Balda, M. A., Martínez Catalán, J. R. and Ayarza Arribas, P.: Syn-collisional extensional
899 collapse parallel to the orogenic trend in a domain of steep tectonics: the Salamanca
900 Detachment Zone (Central Iberian Zone, Spain), *J. Struct. Geol.*, 17(2), 163–182,
901 doi:10.1016/0191-8141(94)E0042-W, 1995.
- 902 Díez Fernández, R. and Arenas, R.: The Late Devonian Variscan suture of the Iberian Massif: A
903 correlation of high-pressure belts in NW and SW Iberia, *Tectonophysics*, 654, 96–100,
904 doi:10.1016/j.tecto.2015.05.001, 2015.
- 905 Díez Fernández, R. and Pereira, M. F.: Extensional orogenic collapse captured by strike-slip
906 tectonics: Constraints from structural geology and UPb geochronology of the Pinhel shear zone
907 (Variscan orogen, Iberian Massif), *Tectonophysics*, 691, 290–310,
908 doi:10.1016/j.tecto.2016.10.023, 2016.
- 909 Díez Fernández, R. and Pereira, M. F.: Strike-slip shear zones of the Iberian Massif: Are they
910 coeval?, *Lithosphere*, 9(5), 726–744, doi:10.1130/L648.1, 2017.
- 911 Díez Fernández, R., Gómez Barreiro, J., Martínez Catalán, J. R. and Ayarza, P.: Crustal
912 thickening and attenuation as revealed by regional fold interference patterns: Ciudad Rodrigo
913 basement area (Salamanca, Spain), *J. Struct. Geol.*, 46, 115–128,
914 doi:10.1016/j.jsg.2012.09.017, 2013.
- 915 Díez Fernández, R., Arenas, R., Pereira, M. F., Sánchez-Martínez, S., Albert, R., Martín Parra,
916 L.-M., Rubio Pascual, F.-J. and Matas, J.: Tectonic evolution of Variscan Iberia: Gondwana–
917 Laurussia collision revisited, *Earth-Sci. Rev.*, 162, 269–292,
918 doi:10.1016/j.earscirev.2016.08.002, 2016.
- 919 Díez-Montes, A.: La Geología del Dominio “Ollo de Sapo” en las comarcas de Sanabria y
920 Terra do Bolo., 2006.
- 921 Díez-Montes, A., Martínez-Catalán, J. R. R. and Bellido-Mulas, F.: Role of the Ollo de Sapo
922 massive felsic volcanism of NW Iberia in the Early Ordovician dynamics of northern Gondwana,
923 *Gondwana Res.*, 17(2–3), 363–376, doi:10.1016/j.gr.2009.09.001, 2010.



- 924 Domeier, M. and Torsvik, T. H.: Plate tectonics in the late Paleozoic, *Geosci. Front.*, 5(3), 303–
925 350, doi:10.1016/j.gsf.2014.01.002, 2014.
- 926 Edel, J. B., Schulmann, K., Lexa, O. and Lardeaux, J. M.: Late Palaeozoic palaeomagnetic and
927 tectonic constraints for amalgamation of Pangea supercontinent in the European Variscan belt,
928 *Earth-Sci. Rev.*, 177(September 2017), 589–612, doi:10.1016/j.earscirev.2017.12.007, 2018.
- 929 Eduard Suess: *Das Antlitz der Erde*, F. Tempsky; [etc., etc.]. [online] Available from:
930 <http://archive.org/details/dasantlitzderer02suesgoog> (Accessed 12 March 2020), 1892.
- 931 Eichelberger, N. and McQuarrie, N.: Kinematic reconstruction of the Bolivian orocline,
932 *Geosphere*, 11(2), 445–462, doi:10.1130/GES01064.1, 2015.
- 933 Escuder Viruete, J., Arenas, R. and Catalán, J. R. M.: Tectonothermal evolution associated with
934 Variscan crustal extension in the Tormes Gneiss Dome (NW Salamanca, Iberian Massif, Spain),
935 *Tectonophysics*, 238(1), 117–138, doi:10.1016/0040-1951(94)90052-3, 1994.
- 936 Fernández-Lozano, J., Pastor-Galán, D., Gutiérrez-Alonso, G. and Franco, P.: New kinematic
937 constraints on the Cantabrian orocline: A paleomagnetic study from the Peñalba and Truchas
938 synclines, NW Spain, *Tectonophysics*, 681, 195–208, doi:10.1016/j.tecto.2016.02.019, 2016.
- 939 Fernández-Lozano, J., Gutiérrez-Alonso, G., Willingshofer, E., Sokoutis, D., Vicente, G. de and
940 Cloetingh, S.: Shaping of intraplate mountain patterns: The Cantabrian orocline legacy in Alpine
941 Iberia, *Lithosphere*, 11(5), 708–721, doi:10.1130/L1079.1, 2019.
- 942 Fernández-Suárez, J., Gutiérrez-Alonso, G., Pastor-Galán, D., Hofmann, M., Murphy, J. B. and
943 Linnemann, U.: The Ediacaran-Early Cambrian detrital zircon record of NW Iberia: Possible
944 sources and paleogeographic constraints, *Int. J. Earth Sci.*, 103(5), 1335–1357,
945 doi:10.1007/s00531-013-0923-3, 2014.
- 946 Fossen, H.: *Structural Geology*, Cambridge University Press., 2016.
- 947 Franke, W., Cocks, L. R. M. and Torsvik, T. H.: The Palaeozoic Variscan oceans revisited,
948 *Gondwana Res.*, 48, 257–284, doi:10.1016/j.gr.2017.03.005, 2017.
- 949 Franke, W., Cocks, L. R. M. and Torsvik, T. H.: Detrital zircons and the interpretation of
950 palaeogeography, with the Variscan Orogeny as an example, *Geol. Mag.*, 157(4), 690–694,
951 doi:10.1017/S0016756819000943, 2020.
- 952 García-Arias, M., Díez-Montes, A., Villaseca, C. and Blanco-Quintero, I. F.: The Cambro-
953 Ordovician Ollo de Sapo magmatism in the Iberian Massif and its Variscan evolution: A review,
954 *Earth-Sci. Rev.*, 176, 345–372, doi:10.1016/j.earscirev.2017.11.004, 2018.
- 955 Gong, Z., Langereis, C. G. and Mullender, T. A. T.: The rotation of Iberia during the Aptian and
956 the opening of the Bay of Biscay, *Earth Planet. Sci. Lett.*, 273(1–2), 80–93, 2008.
- 957 Gozalo, R., Liñán, E., Vintaned, J. A. G., Eugenia, M., Álvarez, D., Martorell, J. B. C., Zamora,
958 S., Esteve, J. and Mayoral, E.: The Cambrian of the Cadenas Ibéricas (ne Spain) and Its
959 Trilobites., n.d.
- 960 Greco, K. D., Johnston, S. T., Gutiérrez-Alonso, G., Shaw, J. and Lozano, J. F.: Interference



- 961 folding and orocline implications: A structural study of the Ponga Unit, Cantabrian orocline,
962 northern Spain, *Lithosphere*, 8(6), 757–768, doi:10.1130/L576.1, 2016.
- 963 Gutiérrez Alonso, G.: Estratigrafía y Tectónica., in Memoria del Mapa Geológico de España
964 1:50000, Hoja de Mora (680), IGME, Madrid. [online] Available from:
965 <http://info.igme.es/cartografiadigital/datos/magna50/memorias/MMagna0658.pdf>, 2009.
- 966 Gutiérrez-Alonso, G.: El Antiforme del Narcea y su relación con los mantos occidentales de la
967 Zona Cantábrica., 1992.
- 968 Gutiérrez-Alonso, G.: Strain partitioning in the footwall of the Somiedo Nappe: Structural
969 evolution of the Narcea Tectonic window, NW Spain, *J. Struct. Geol.*, 18(10), 1217–1229, 1996.
- 970 Gutiérrez-Alonso, G., Fernández-Suárez, J. and Weil, A. B.: Orocline triggered lithospheric
971 delamination, in Special Paper 383: Orogenic curvature: Integrating paleomagnetic and
972 structural analyses, vol. 383, edited by A. B. Weil and A. Sussman, pp. 121–130, Geological
973 Society of America, Boulder., 2004.
- 974 Gutiérrez-Alonso, G., Fernández-Suárez, J., Weil, A. B., Brendan Murphy, J., Damian Nance,
975 R., Corf, F. and Johnston, S. T.: Self-subduction of the Pangaeon global plate, *Nat. Geosci.*,
976 1(8), 549–553, doi:10.1038/ngeo250, 2008a.
- 977 Gutiérrez-Alonso, G., Murphy, J. B. B., Fernández-Suárez, J. and Hamilton, M. A. A.: Rifting
978 along the northern Gondwana margin and the evolution of the Rheic Ocean: A Devonian age for
979 the El Castillo volcanic rocks (Salamanca, Central Iberian Zone), *Tectonophysics*, 461(1–4),
980 157–165, doi:10.1016/j.tecto.2008.01.013, 2008b.
- 981 Gutiérrez-Alonso, G., Fernández-Suárez, J., Jeffries, T. E. T. E. E., Johnston, S. T., Pastor-
982 Galán, D., Murphy, J. B. B., Franco, M. P. P., Gonzalo, J. C. C.: Diachronous post-orogenic
983 magmatism within a developing orocline in Iberia, *European Variscides*, *Tectonics*, 30(5), 17
984 PP.-17 PP., doi:10.1029/2010TC002845, 2011a.
- 985 Gutiérrez-Alonso, G., Murphy, J. B., Fernández-Suárez, J., Weil, A. B., Franco, M. P., Gonzalo,
986 J. C.: Lithospheric delamination in the core of Pangea: Sm-Nd insights from the Iberian mantle,
987 *Geology*, 39(2), 155–158, doi:10.1130/G31468.1, 2011b.
- 988 Gutiérrez-Alonso, G., Collins, A. S., Fernández-Suárez, J., Pastor-Galán, D., González-Clavijo,
989 E., Jourdan, F., Weil, A. B. and Johnston, S. T.: Dating of lithospheric buckling: $^{40}\text{Ar}/^{39}\text{Ar}$ ages
990 of syn-orocline strike-slip shear zones in northwestern Iberia, *Tectonophysics*, 643, 44–54,
991 doi:10.1016/j.tecto.2014.12.009, 2015.
- 992 Gutiérrez-Alonso, G., Fernández-Suárez, J., López-Carmona, A. and Gärtner, A.: Exhuming a
993 cold case: The early granodiorites of the northwest Iberian Variscan belt—A Visean magmatic
994 flare-up?, *Lithosphere*, 10(2), 194–216, doi:10.1130/L706.1, 2018.
- 995 Gutiérrez-Marco, J. C., Sá, A. A., García-Bellido, D. C. and Rábano, I.: The Bohemo-Iberian
996 regional chronostratigraphical scale for the Ordovician System and palaeontological correlations
997 within South Gondwana, *Lethaia*, 50(2), 258–295, doi:10.1111/let.12197, 2017.
- 998 Gutiérrez-Marco, J. C., Piçarra, J. M., Meireles, C. A., Cózar, P., García-Bellido, D. C., Pereira,
999 Z., Vaz, N., Pereira, S., Lopes, G., Oliveira, J. T., Quesada, C., Zamora, S., Esteve, J.,



- 1000 Colmenar, J., Bernárdez, E., Coronado, I., Lorenzo, S., Sá, A. A., Dias da Silva, Í., González-
1001 Clavijo, E., Díez-Montes, A. and Gómez-Barreiro, J.: Early Ordovician–Devonian Passive
1002 Margin Stage in the Gondwanan Units of the Iberian Massif, in *The Geology of Iberia: A*
1003 *Geodynamic Approach*, edited by C. Quesada and J. T. Oliveira, pp. 75–98, Springer
1004 International Publishing, Cham., 2019.
- 1005 Hindle, D., Besson, O. and Burkhard, M.: A model of displacement and strain for arc-shaped
1006 mountain belts applied to the Jura arc, *J. Struct. Geol.*, 22(9), 1285–1296, doi:10.1016/S0191-
1007 8141(00)00038-9, 2000.
- 1008 van Hinsbergen, D. J. J., Torsvik, T. H., Schmid, S. M., Mañenco, L. C., Maffione, M., Vissers, R.
1009 L. M., Gürer, D. and Spakman, W.: Orogenic architecture of the Mediterranean region and
1010 kinematic reconstruction of its tectonic evolution since the Triassic, *Gondwana Res.*, 81, 79–
1011 229, doi:10.1016/j.gr.2019.07.009, 2020.
- 1012 Hirt, A. M., Lowrie, W., Julivert, M., Arboleya, M. L., Lowric, A. M. H. W. and Arboleya, M. L.:
1013 Paleomagnetic results in support of a model for the origin of the Asturian arc, *Tectonophysics*,
1014 213(3–4), 321–339, 1992.
- 1015 Hnat, J. S. and van der Pluijm, B. A.: Foreland signature of indenter tectonics: Insights from
1016 calcite twinning analysis in the Tennessee salient of the Southern Appalachians, USA,
1017 *Lithosphere*, 3(5), 317–327, doi:10.1130/L151.1, 2011.
- 1018 Holmes, A.: A review of the continental drift hypothesis., *Min. Mag.*, 40, 205–209, 1929.
- 1019 Huang, W., Lippert, P. C., Zhang, Y., Jackson, M. J., Dekkers, M. J., Li, J., Hu, X., Zhang, B.,
1020 Guo, Z. and van Hinsbergen, D. J. J. J.: Remagnetization of carbonate rocks in southern Tibet:
1021 Perspectives from rock magnetic and petrographic investigations, *J. Geophys. Res. Solid Earth*,
1022 122(4), 2434–2456, doi:10.1002/2017JB013987, 2017.
- 1023 Izquierdo-Llavall, E., Sainz, A. C., Oliva-Urcia, B., Burmester, R., Pueyo, E. L. and Housen, B.:
1024 Multi-episodic remagnetization related to deformation in the Pyrenean Internal Sierras,
1025 *Geophys. J. Int.*, 201(2), 891–914, doi:10.1093/gji/ggv042, 2015.
- 1026 Izquierdo-Llavall, E., Casas-Sainz, A. M., Oliva-Urcia, B., Villalaín, J. J., Pueyo, E. and
1027 Scholger, R.: Rotational Kinematics of Basement Antiformal Stacks: Paleomagnetic Study of the
1028 Western Noguera Zone (Central Pyrenees), *Tectonics*, 37(10), 3456–3478,
1029 doi:10.1029/2018TC005153, 2018.
- 1030 Izquierdo-Llavall, E., Ayala, C., Pueyo, E. L., Casas-Sainz, A. M., Oliva-Urcia, B., Rubio, F.,
1031 Rodríguez-Pintó, A., Rey-Moral, C., Mediato, J. F. and García-Crespo, J.: Basement-Cover
1032 Relationships and Their Along-Strike Changes in the Linking Zone (Iberian Range, Spain): A
1033 Combined Structural and Gravimetric Study, *Tectonics*, 38(8), 2934–2960,
1034 doi:10.1029/2018TC005422, 2019.
- 1035 Jabaloy-Sánchez, A., Talavera, C., Gómez-Pugnaire, M. T., López-Sánchez-Vizcaíno, V.,
1036 Vázquez-Vílchez, M., Rodríguez-Peces, M. J. and Evans, N. J.: U-Pb ages of detrital zircons
1037 from the Internal Betics: A key to deciphering paleogeographic provenance and tectono-
1038 stratigraphic evolution, *Lithos*, 318–319, 244–266, doi:10.1016/j.lithos.2018.07.026, 2018.
- 1039 Jackson, M.: Diagenetic sources of stable remanence in remagnetized paleozoic cratonic



- 1040 carbonates: A rock magnetic study, *J. Geophys. Res. Solid Earth*, 95(B3), 2753–2761,
1041 doi:10.1029/JB095iB03p02753, 1990.
- 1042 Jacques, D., Muchez, P. and Sintubin, M.: Superimposed folding and W-Sn vein-type
1043 mineralisation in the Central Iberian Zone associated with late-Variscan oroclinal buckling: A
1044 structural analysis from the Regoufe area (Portugal), *Tectonophysics*, 742–743, 66–83,
1045 doi:10.1016/j.tecto.2018.05.021, 2018a.
- 1046 Jacques, D., Vieira, R., Muchez, P. and Sintubin, M.: Transpressional folding and associated
1047 cross-fold jointing controlling the geometry of post-orogenic vein-type W-Sn mineralization:
1048 examples from Minas da Panasqueira, Portugal, *Miner. Deposita*, 53(2), 171–194,
1049 doi:10.1007/s00126-017-0728-6, 2018b.
- 1050 Johnston, S. T.: The Great Alaskan Terrane Wreck: Reconciliation of paleomagnetic and
1051 geological data in the Northern Cordillera, *Earth Planet. Sci. Lett.*, 193(3–4), 259–272,
1052 doi:10.1016/S0012-821X(01)00516-7, 2001.
- 1053 Johnston, S. T., Weil, A. B. and Gutiérrez-Alonso, G.: Oroclines: Thick and thin, *GSA Bull.*,
1054 125(5–6), 643–663, doi:10.1130/B30765.1, 2013.
- 1055 Julivert, M.: L'évolution structurale de l'Arc Asturien, Paris., 1971.
- 1056 Julivert, M. and Arboleya, M. L.: A geometrical and kinematical approach to the nappe structure
1057 in an arcuate fold belt: the Cantabrian nappes (Hercynian chain, NW Spain), *J. Struct. Geol.*,
1058 6(5), 499–519, doi:10.1016/0191-8141(84)90061-0, 1984.
- 1059 Julivert, M. and Marcos, A.: superimposed folding under flexural conditions in the Cantabrian
1060 Zone (Hercynian Cordillera, Northwest Spain), *Am. J. Sci.*, 273(5), 353–375,
1061 doi:10.2475/ajs.273.5.353, 1973.
- 1062 Julivert, M., Fontboté, J. M., Ribeiro, A. and Nabais Conde, L. E.: Mapa Tectónico de la
1063 Península Ibérica y Baleares E: 1: 1.000. 000 y memoria explicativa, *Publ IGME*, 113, 1974.
- 1064 Julivert, M., Vegas, R., Roiz, J. M. and Martínez Rius, A.: Laestructura de la extension SE de la
1065 Zona Centro-Iberica con metamorfismo de bajo grado, *Rios-Geol. Esp. I*, 339–380, 1983.
- 1066 Keppie, F.: How subduction broke up Pangaea with implications for the supercontinent cycle,
1067 *Geol. Soc. Lond. Spec. Publ.*, 424(1), 265–288, doi:10.1144/SP424.8, 2016.
- 1068 Kirsch, M., Keppie, J. D., Murphy, J. B. and Solari, L. A.: Permian-Carboniferous arc
1069 magmatism and basin evolution along the western margin of Pangea: Geochemical and
1070 geochronological evidence from the eastern Acatlan Complex, southern Mexico, *Geol. Soc. Am.
1071 Bull.*, 124(9–10), 1607–1628, doi:10.1130/B30649.1, 2012.
- 1072 Kollmeier, J. M., van der Pluijm, B. A. and Van der Voo, R.: Analysis of Variscan dynamics;
1073 early bending of the Cantabria-Asturias Arc, northern Spain, *Earth Planet. Sci. Lett.*, 181(1–2),
1074 203–216, doi:10.1016/S0012-821X(00)00203-X, 2000.
- 1075 Kroner, U. and Romer, R. L. L.: Two plates — Many subduction zones: The Variscan orogeny
1076 reconsidered, *Gondwana Res.*, 24(1), 298–329, doi:10.1016/j.gr.2013.03.001, 2013.



- 1077 Li, P. and Rosenbaum, G.: Does the Manning Orocline exist? New structural evidence from the
1078 inner hinge of the Manning Orocline (eastern Australia), *Gondwana Res.*, 25(4), 1599–1613,
1079 doi:10.1016/j.gr.2013.06.010, 2014.
- 1080 Li, P., Sun, M., Rosenbaum, G., Yuan, C., Safonova, I., Cai, K., Jiang, Y. and Zhang, Y.:
1081 Geometry, kinematics and tectonic models of the Kazakhstan Orocline, Central Asian Orogenic
1082 Belt, *J. Asian Earth Sci.*, 153(July 2017), 42–56, doi:10.1016/j.jseaes.2017.07.029, 2018.
- 1083 Li, P.-F., Rosenbaum, G. and Rubatto, D.: Triassic asymmetric subduction rollback in the
1084 southern New England Orogen (eastern Australia): the end of the Hunter-Bowen Orogeny, *Aust.*
1085 *J. Earth Sci.*, 59(6), 965–981, doi:10.1080/08120099.2012.696556, 2012.
- 1086 López-Carmona, A., Abati, J., Pitra, P. and Lee, J. K. W.: Retrogressed lawsonite blueschists
1087 from the NW Iberian Massif: P–T–t constraints from thermodynamic modelling and ⁴⁰Ar/³⁹Ar
1088 geochronology, *Contrib. Mineral. Petrol.*, 167(3), 987–987, doi:10.1007/s00410-014-0987-5,
1089 2014.
- 1090 López-Moro, F. J., López-Plaza, M., Gutiérrez-Alonso, G., Fernández-Suárez, J., López-
1091 Carmona, A., Hofmann, M. and Romer, R. L.: Crustal melting and recycling: geochronology and
1092 sources of Variscan syn-kinematic anatectic granitoids of the Tormes Dome (Central Iberian
1093 Zone). A U–Pb LA-ICP-MS study, *Int. J. Earth Sci.*, 107(3), 985–1004, doi:10.1007/s00531-017-
1094 1483-8, 2018.
- 1095 Lotze, F.: Zur gliederung der Variszichen der Iberischen Meseta., *Geotektonische Forschungen*,
1096 6, 78–92, 1945.
- 1097 Macaya, J., González-Lodeiro, F., Martínez-Catalán, J. R. and Alvarez, F.: Continuous
1098 deformation, ductile thrusting and backfolding of cover and basement in the Sierra de
1099 Guadarrama, Hercynian orogen of central Spain, *Tectonophysics*, 191(3), 291–309,
1100 doi:10.1016/0040-1951(91)90063-X, 1991.
- 1101 Maffione, M., Speranza, F. and Faccenna, C.: Bending of the Bolivian orocline and growth of the
1102 central Andean plateau: Paleomagnetic and structural constraints from the Eastern Cordillera
1103 (22–24°S, NW Argentina), *Tectonics*, 28, 23 PP.-23 PP., doi:10.1029/2008TC002402, 2009.
- 1104 Marcos, A. and Pulgar, J. A. A.: An Approach to the tectonostratigraphic evolution of the
1105 Cantabrian foreland thrust and fold belt, Hercynian Cordillera of NW Spain, *Neues Jahrb. Geol.*
1106 *Palaontologie-Abh.*, 163(2), 256–260, 1982.
- 1107 Marcos, A., Pérez-Estaún, A., Martínez Catalán, J. R. and Gutiérrez-Marco, J. C.: *Estratigrafía y*
1108 *Paleogeografía. Zona Asturoccidental-Leonesa*, 2004.
- 1109 Marshak, S.: KINEMATICS OF OROCLINE AND ARC FORMATION IN THIN-SKINNED
1110 OROGENS, *Tectonics*, 7(1), 73–86, 1988.
- 1111 Marshak, S.: Salients, Recesses, Arcs, Oroclines, and Syntaxes — A Review of Ideas
1112 Concerning the Formation of Map-view Curves in Fold-thrust Belts, *Thrust Tecton. Hydrocarb.*
1113 *Syst. AAPG Mem.* 82, 82(1893), 131–156, 2004.
- 1114 Martín-Algarra, A., García-Casco, A., Gómez-Pugnaire, M. T., Jabaloy-Sánchez, A., Laborda-
1115 López, C., López Sánchez-Vizcaíno, V., Mazzoli, S., Navas-Parejo, P., Perrone, V., Rodríguez-



- 1116 Cañero, R. and Sánchez-Navas, A.: Paleozoic Basement and Pre-Alpine History of the Betic
1117 Cordillera, in *The Geology of Iberia: A Geodynamic Approach*, edited by C. Quesada and J. T.
1118 Oliveira, pp. 261–305, Springer International Publishing, Cham., 2019.
- 1119 Martínez Catalán, J. R.: Are the oroclines of the Variscan belt related to late Variscan strike–slip
1120 tectonics?, *Terra Nova*, 23(4), 241–247, doi:10.1111/j.1365-3121.2011.01005.x, 2011.
- 1121 Martínez Catalán, J. R.: The Central Iberian arc, an orocline centered in the Iberian Massif and
1122 some implications for the Variscan belt, *Int. J. Earth Sci.*, 101(5), 1–16, doi:10.1007/s00531-
1123 011-0715-6, 2012.
- 1124 Martínez Catalán, J. R., Rodríguez, M. P. H., Alonso, P. V., Pérez-Estaun, A. and Lodeiro, F. G.:
1125 Lower Paleozoic extensional tectonics in the limit between the West Asturian-Leonese and
1126 Central Iberian Zones of the Variscan Fold-Belt in NW Spain, *Geol. Rundsch.*, 81(2), 545–560,
1127 doi:10.1007/BF01828614, 1992.
- 1128 Martínez Catalán, J. R., Martínez Poyatos, D. and Bea, F.: Zona Centroibérica, *Geol. Esp.*, 68–
1129 133, 2004.
- 1130 Martínez Catalán, J. R., Arenas, R., Abati, J., Martínez, S. S., García, F. D., Suárez, J. F.,
1131 Cuadra, P. G., Castiñeiras, P., Barreiro, J. G., Montes, A. D., Clavijo, E. G., Pascual, F. J. R.,
1132 Andonaegui, P., Jeffries, T. E., Alcock, J. E., Fernández, R. D. and Carmona, A. L.: A rootless
1133 suture and the loss of the roots of a mountain chain: The Variscan belt of NW Iberia, *Comptes
1134 Rendus Geosci.*, 341(2), 114–126, doi:10.1016/j.crte.2008.11.004, 2009.
- 1135 Martínez Catalán, J. R., Rubio Pascual, F. J., Diez Montes, A., Diez Fernández, R., Gomez
1136 Barreiro, J., Dias da Silva, I., Gonzalez Clavijo, E., Ayarza, P., Alcock, J. E., Montes, A. D.,
1137 Fernandez, R. D., Barreiro, J. G., Dias da Silva, I., Clavijo, E. G., Ayarza, P., Alcock, J. E., Diez
1138 Montes, A., Diez Fernández, R., Gomez Barreiro, J., Dias da Silva, I., Gonzalez Clavijo, E.,
1139 Ayarza, P., Alcock, J. E., Montes, A. D., Fernandez, R. D., Barreiro, J. G., Dias da Silva, I.,
1140 Clavijo, E. G., Ayarza, P. and Alcock, J. E.: The late Variscan HT/LP metamorphic event in NW
1141 and Central Iberia: relationships to crustal thickening, extension, orocline development and
1142 crustal evolution, *Geol. Soc. Lond. Spec. Publ.*, 405(1), 225–247, doi:10.1144/SP405.1, 2014.
- 1143 Martínez Catalán, J. R., Aerden, D. G. A. M. and Carreras, J.: The “Castilian bend” of Rudolf
1144 Staub (1926): historical perspective of a forgotten orocline in Central Iberia, *Swiss J. Geosci.*,
1145 108(2–3), 289–303, doi:10.1007/s00015-015-0202-3, 2015.
- 1146 Martínez Catalán, J. R., Gómez Barreiro, J., Dias da Silva, Í., Chichorro, M., López-Carmona,
1147 A., Castiñeiras, P., Abati, J., Andonaegui, P., Fernández-Suárez, J., González Cuadra, P. and
1148 Benítez-Pérez, J. M.: Variscan Suture Zone and Suspect Terranes in the NW Iberian Massif:
1149 Allochthonous Complexes of the Galicia-Trás os Montes Zone (NW Iberia), in *The Geology of
1150 Iberia: A Geodynamic Approach*, edited by C. Quesada and J. T. Oliveira, pp. 99–130, Springer
1151 International Publishing, Cham., 2019.
- 1152 Martínez-Catalán, J. R.: A non-cylindrical model for the northwest Iberian allochthonous
1153 terranes and their equivalents in the Hercynian belt of Western Europe, *Tectonophysics*, 179(3–
1154 4), 253–272, doi:10.1016/0040-1951(90)90293-H, 1990.
- 1155 McWilliams, C. K., Kunk, M. J., Wintsch, R. P. and Bish, D. L.: Determining ages of multiple
1156 muscovite-bearing foliations in phyllonites using the $^{40}\text{Ar}/^{39}\text{Ar}$ step heating method:



- 1157 Applications to the alleghanian orogeny in central new England, *Am. J. Sci.*, 313(10), 996–1016,
1158 doi:10.2475/10.2013.02, 2013.
- 1159 Meijers, M. J. M., Smith, B., Pastor-Galán, D., Degenaar, R., Sadradze, N., Adamia, S.,
1160 Sahakyan, L., Avagyan, A., Sosson, M., Rolland, Y., Langereis, C. G. and Müller, C.:
1161 Progressive orocline formation in the Eastern Pontides-Lesser Caucasus, *Geol. Soc. Spec.*
1162 *Publ.*, 428(1), doi:10.1144/SP428.8, 2017.
- 1163 Merino-Tomé, O. A., Bahamonde, J. R., Colmenero, J. R., Heredia, N., Villa, E. and Farias, P.:
1164 Emplacement of the Cuera and Picos de Europa imbricate system at the core of the Iberian-
1165 Armorican arc (Cantabrian zone, north Spain): New precisions concerning the timing of arc
1166 closure, *Bull. Geol. Soc. Am.*, 121(5–6), 729–751, doi:10.1130/B26366.1, 2009.
- 1167 Molina Garza, R. S. and Zijdeveld, J. D. a.: Paleomagnetism of Paleozoic strata, Brabant and
1168 Ardennes Massifs, Belgium: Implications of prefolding and postfolding Late Carboniferous
1169 secondary magnetizations for European apparent polar wander, *J. Geophys. Res.*, 101(B7),
1170 15799–15799, doi:10.1029/96JB00325, 1996.
- 1171 Moral, B. del and Sarmiento, G. N.: Conodontos del Katiense (Ordovícico Superior) del sector
1172 meridional de la Zona Centroibérica (España), *Rev. Esp. Micropaleontol.*, 40(3), 169–245, 2008.
- 1173 Munha, J.: Metamorphic Evolution of the South Portuguese/Pulo Do Lobo Zone, in *Pre-*
1174 *Mesozoic Geology of Iberia*, edited by R. D. Dallmeyer and E. M. Garcia, pp. 363–368,
1175 Springer, Berlin, Heidelberg., 1990.
- 1176 Munha, J., Barriga, F. J. a. S. and Kerrich, R.: High 18 O ore-forming fluids in volcanic-hosted
1177 base metal massive sulfide deposits; geologic, 18 O/ 16 O, and D/H evidence from the Iberian
1178 pyrite belt; Crandon, Wisconsin; and Blue Hill, Maine, *Econ. Geol.*, 81(3), 530–552, doi:10.2113/
1179 gsecongeo.81.3.530, 1986.
- 1180 Murphy, J. B., Gutierrez-Alonso, G., Fernandez-Suarez, J. and Braid, J. A.: Probing crustal and
1181 mantle lithosphere origin through Ordovician volcanic rocks along the Iberian passive margin of
1182 Gondwana, *Tectonophysics*, 461(1–4), 166–180, 2008.
- 1183 Nance, R. D., Gutiérrez-Alonso, G., Keppie, J. D., Linnemann, U., Murphy, J. B., Quesada, C.,
1184 Strachan, R. A. and Woodcock, N. H.: Evolution of the Rheic Ocean, *Gondwana Res.*, 17(2–3),
1185 194–222, doi:10.1016/j.gr.2009.08.001, 2010.
- 1186 Oliveira, J. T., Quesada, C., Pereira, Z., Matos, J. X., Solá, A. R., Rosa, D., Albardeiro, L., Díez-
1187 Montes, A., Morais, I., Inverno, C., Rosa, C. and Relvas, J.: South Portuguese Terrane: A
1188 Continental Affinity Exotic Unit, in *The Geology of Iberia: A Geodynamic Approach*, edited by C.
1189 Quesada and J. T. Oliveira, pp. 173–206, Springer International Publishing, Cham., 2019a.
- 1190 Oliveira, J. T., González-Clavijo, E., Alonso, J., Armendáriz, M., Bahamonde, J. R., Braid, J. A.,
1191 Colmenero, J. R., Dias da Silva, Í., Fernandes, P., Fernández, L. P., Gabaldón, V., Jorge, R. S.,
1192 Machado, G., Marcos, A., Merino-Tomé, Ó., Moreira, N., Murphy, J. B., Pinto de Jesus, A.,
1193 Quesada, C., Rodrigues, B., Rosales, I., Sanz-López, J., Suárez, A., Villa, E., Piçarra, J. M. and
1194 Pereira, Z.: Synorogenic Basins, in *The Geology of Iberia: A Geodynamic Approach*, edited by
1195 C. Quesada and J. T. Oliveira, pp. 349–429, Springer International Publishing, Cham., 2019b.
- 1196 P. Farias, G. G.: Aportaciones al conocimiento de la litoestratigrafía y estructura de Galicia



- 1197 Central, Mem. Fac. Ciênc. Universidade Porto, 411–431, 1987.
- 1198 Palero-Fernández, F. J., Martin-Izard, A., Zarzalejos Prieto, M. and Mansilla-Plaza, L.:
1199 Geological context and plumbotectonic evolution of the giant Almadén Mercury Deposit, Ore
1200 Geol. Rev., 64, 71–88, doi:10.1016/j.oregeorev.2014.06.013, 2015.
- 1201 Parés, J. M. and Van der Voo, R.: Paleozoic paleomagnetism of Almaden, Spain: A cautionary
1202 note, J. Geophys. Res., 97(B6), 9353–9356, doi:10.1029/91JB03073, 1992.
- 1203 Parés, J. M., Van der Voo, R., Stamatakos, J. and Pérez-Estaún, A.: Remagnetizations and
1204 postfolding oroclinal rotations in the Cantabrian/Asturian arc, northern Spain, Tectonics, 13(6),
1205 1461–1471, doi:10.1029/94TC01871, 1994.
- 1206 Pastor-Galán, D., Gutiérrez-Alonso, G., Meere, P. A. and Mulchrone, K. F.: Factors affecting
1207 finite strain estimation in low-grade, low-strain clastic rocks, J. Struct. Geol., 31(12), 1586–1596,
1208 doi:10.1016/j.jsg.2009.08.005, 2009.
- 1209 Pastor-Galán, D., Gutiérrez-Alonso, G. and Weil, A. B.: Orocline timing through joint analysis:
1210 Insights from the Ibero-Armorican Arc, Tectonophysics, 507(1), 31–46,
1211 doi:10.1016/j.tecto.2011.05.005, 2011.
- 1212 Pastor-Galán, D., Gutiérrez-Alonso, G., Zulauf, G. and Zanella, F.: Analogue modeling of
1213 lithospheric-scale orocline buckling: Constraints on the evolution of the Iberian-Armorican arc,
1214 Bull. Geol. Soc. Am., 124(7–8), doi:10.1130/B30640.1, 2012a.
- 1215 Pastor-Galán, D., Gutiérrez-Alonso, G., Mulchrone, K. F. and Huerta, P.: Conical folding in the
1216 core of an orocline. A geometric analysis from the Cantabrian Arc (Variscan Belt of NW Iberia),
1217 J. Struct. Geol., 39, 210–223, doi:10.1016/j.jsg.2012.02.010, 2012b.
- 1218 Pastor-Galán, D., Gutiérrez-Alonso, G., Murphy, J. B. B., Fernández-Suárez, J., Hofmann, M.
1219 and Linnemann, U.: Provenance analysis of the Paleozoic sequences of the northern
1220 Gondwana margin in NW Iberia: Passive margin to Variscan collision and orocline development,
1221 Gondwana Res., 23(3), 1089–1103, doi:10.1016/j.gr.2012.06.015, 2013a.
- 1222 Pastor-Galán, D., Gutiérrez-Alonso, G., Fernández-Suárez, J., Murphy, J. B. and Nieto, F.:
1223 Tectonic evolution of NW Iberia during the Paleozoic inferred from the geochemical record of
1224 detrital rocks in the Cantabrian Zone, Lithos, 182–183, 221–228,
1225 doi:10.1016/j.lithos.2013.09.007, 2013b.
- 1226 Pastor-Galán, D., Martín-Merino, G. and Corrochano, D.: Timing and structural evolution in the
1227 limb of an orocline: The Pisuerga-Carrión Unit (southern limb of the Cantabrian Orocline, NW
1228 Spain), Tectonophysics, 622, 110–121, doi:10.1016/j.tecto.2014.03.004, 2014.
- 1229 Pastor-Galán, D., Ursem, B., Meere, P. A. and Langereis, C.: Extending the Cantabrian
1230 Orocline to two continents (from Gondwana to Laurussia). Paleomagnetism from South Ireland,
1231 Earth Planet. Sci. Lett., 432, doi:10.1016/j.epsl.2015.10.019, 2015a.
- 1232 Pastor-Galán, D., Groenewegen, T., Brouwer, D., Krijgsman, W., Dekkers, M. J., Pastor-galán,
1233 D., Groenewegen, T., Brouwer, D., Krijgsman, W. and Dekkers, M. J.: One or two oroclinal in
1234 the Variscan orogen of Iberia? Implications for Pangea amalgamation, Geology, 43(6), 527–
1235 530, doi:10.1130/G36701.1, 2015b.



- 1236 Pastor-Galán, D., Dekkers, M. J., Gutiérrez-Alonso, G., Brouwer, D., Groenewegen, T.,
1237 Krijgsman, W., Fernández-Lozano, J., Yenes, M. and Álvarez-Lobato, F.: Paleomagnetism of
1238 the Central Iberian curve's putative hinge: Too many oroclines in the Iberian Variscides,
1239 *Gondwana Res.*, 39, 96–113, doi:10.1016/j.gr.2016.06.016, 2016.
- 1240 Pastor-Galán, D., Mulchrone, K. F., Koymans, M. R. , van Hinsbergen, D. J. J. and Langereis,
1241 C. G. : Bootstrapped total least squares orocline test: A robust method to quantify vertical-axis
1242 rotation patterns in orogens, with examples from the Cantabrian and Aegean oroclines,
1243 *Lithosphere*, 9(3), L547.1-L547.1, doi:10.1130/L547.1, 2017a.
- 1244 Pastor-Galán, D., Gutiérrez-Alonso, G., Dekkers, M. J. M. J. and Langereis, C. G.:
1245 Paleomagnetism in Extremadura (Central Iberian zone, Spain) Paleozoic rocks: extensive
1246 remagnetizations and further constraints on the extent of the Cantabrian orocline, *J. Iber. Geol.*,
1247 43(4), 583–600, doi:10.1007/s41513-017-0039-x, 2017b.
- 1248 Pastor-Galán, D., Pueyo, E. L., Diederer, M., García-Lasanta, C. and Langereis, C. G.: Late
1249 Paleozoic Iberian Orocline(s) and the Missing Shortening in the Core of Pangea.
1250 Paleomagnetism From the Iberian Range, *Tectonics*, 37(10), 3877–3892,
1251 doi:10.1029/2018TC004978, 2018.
- 1252 Pastor-Galán, D., Nance, R. D., Murphy, J. B. and Spencer, C. J.: Supercontinents: myths,
1253 mysteries, and milestones, *Geol. Soc. Lond. Spec. Publ.*, 470, 39–64, doi:10.1144/SP470.16,
1254 2019a.
- 1255 Pastor-Galán, D., Dias da Silva, Í. F., Groenewegen, T. and Krijgsman, W.: Tangled up in folds:
1256 tectonic significance of superimposed folding at the core of the Central Iberian curve (West
1257 Iberia), *Int. Geol. Rev.*, 61(2), 240–255, doi:10.1080/00206814.2017.1422443, 2019b.
- 1258 Pereira, I., Dias, R., Bento, T. and Mata, J.: Exhumation of a migmatite complex along a
1259 transpressive shear zone : inferences from the Variscan Juzbado – Penalva do Castelo Shear
1260 Zone (Central Iberian Zone), *J. Geol. Soc.*, doi:10.1144/jgs2016-159, 2017.
- 1261 Pereira, M. F., Chichorro, M., Silva, J. B., Ordóñez-Casado, B., Lee, J. K. W. W. and Williams, I.
1262 S.: Early carboniferous wrenching, exhumation of high-grade metamorphic rocks and basin
1263 instability in SW Iberia: Constraints derived from structural geology and U–Pb and 40Ar–39Ar
1264 geochronology, *Tectonophysics*, 558, 28–44, doi:10.1016/j.tecto.2012.06.020, 2012.
- 1265 Pereira, M. F., Díez Fernández, R., Gama, C., Hofmann, M., Gärtner, A. and Linnemann, U.: S-
1266 type granite generation and emplacement during a regional switch from extensional to
1267 contractional deformation (Central Iberian Zone, Iberian autochthonous domain, Variscan
1268 Orogeny), *Int. J. Earth Sci.*, 107(1), 251–267, doi:10.1007/s00531-017-1488-3, 2018.
- 1269 Pérez-Cáceres, I., Poyatos, D. M., Simancas, J. F. and Azor, A.: The elusive nature of the
1270 Rhenish Ocean suture in SW Iberia, *Tectonics*, 34(12), 2429–2450, doi:10.1002/2015TC003947,
1271 2015.
- 1272 Pérez-Cáceres, I., Simancas, J. F., Martínez Poyatos, D., Azor, A. and González Lodeiro, F.:
1273 Oblique collision and deformation partitioning in the SW Iberian Variscides, *Solid Earth*, 7(3),
1274 857–872, doi:https://doi.org/10.5194/se-7-857-2016, 2016.
- 1275 Pérez-Cáceres, I., Martínez Poyatos, D., Simancas, J. F. and Azor, A.: Testing the Avalonian



- 1276 affinity of the South Portuguese Zone and the Neoproterozoic evolution of SW Iberia through
1277 detrital zircon populations, *Gondwana Res.*, 42, 177–192, doi:10.1016/j.gr.2016.10.010, 2017.
- 1278 Pérez-Cáceres, I., Martínez Poyatos, D. J., Vidal, O., Beyssac, O., Nieto, F., Simancas, J. F.,
1279 Azor, A. and Bourdelle, F.: Deciphering the metamorphic evolution of the Pulo do Lobo
1280 metasedimentary domain (SW Iberian Variscides), *Solid Earth*, 11(2), 469–488,
1281 doi:https://doi.org/10.5194/se-11-469-2020, 2020.
- 1282 Pérez-Estaún, A., Bastida, F., Alonso, J. L., Marquinez, J., Aller, J., Alvarezmarron, J., Marcos,
1283 A. and Pulgar, J. A.: A THIN-SKINNED TECTONICS MODEL FOR AN ARCUATE FOLD AND
1284 THRUST BELT - THE CANTABRIAN ZONE (VARISCAN IBERO-ARMORICAN ARC),
1285 *Tectonics*, 7(3), 517–537, 1988.
- 1286 Pérez-Estaún, A., Bastida, F., Martínez Catalán, J. R., Gutiérrez-Marco, J. C., Marcos, A. and
1287 Pulgar, J.: Stratigraphy of the West Asturian-Leonese Zone, Springer. [online] Available from:
1288 https://digital.csic.es/handle/10261/30719 (Accessed 6 April 2020), 1990.
- 1289 Pérez-Estaún, A., Martinezcatalan, J. R. and Bastida, F.: CRUSTAL THICKENING AND
1290 DEFORMATION SEQUENCE IN THE FOOTWALL TO THE SUTURE OF THE VARISCAN
1291 BELT OF NORTHWEST SPAIN, *Tectonophysics*, 191(3–4), 243–253, 1991.
- 1292 Perroud, H., Bonhommet, N. and Ribeiro, A.: Paleomagnetism of Late Paleozoic igneous rocks
1293 from southern Portugal, *Geophys. Res. Lett.*, 12(1), 45–48, doi:10.1029/GL012i001p00045,
1294 1985.
- 1295 Perroud, H., Calza, F. and Khattach, D.: Paleomagnetism of the Silurian Volcanism at Almaden,
1296 Southern Spain, *J. Geophys. Res.-Solid Earth Planets*, 96(B2), 1949–1962,
1297 doi:10.1029/90JB02226, 1991.
- 1298 Pin, C., Paquette, J. L., Zalduegui, J. F. S. and Ibarra, J. I. G.: Early Devonian
1299 suprasubduction-zone ophiolite related to incipient collisional processes in the Western
1300 Variscan Belt: The Sierra de Careón unit, Ordenes Complex, Galicia, in *Variscan-Appalachian
1301 dynamics: The building of the late Paleozoic basement*, Geological Society of America., 2002.
- 1302 Pueyo, E. L., Mauritsch, H. J., Gawlick, H.-J., Scholger, R. and Frisch, W.: New evidence for
1303 block and thrust sheet rotations in the central northern Calcareous Alps deduced from two
1304 pervasive remagnetization events, *Tectonics*, 26(5), n/a-n/a, doi:10.1029/2006TC001965, 2007.
- 1305 Pueyo, E. L., Sussman, A. J., Oliva-Urcia, B. and Cifelli, F.: Palaeomagnetism in fold and thrust
1306 belts: Use with caution, *Geol. Soc. Spec. Publ.*, 425(1), 259–276, doi:10.1144/SP425.14, 2016.
- 1307 Quesada, C.: The Ossa-Morena Zone of the Iberian Massif: a tectonostratigraphic approach to
1308 its evolution, *Z. Dtsch. Ges. Für Geowiss.*, 585–595, doi:10.1127/1860-1804/2006/0157-0585,
1309 2006.
- 1310 Quesada, C. and Dallmeyer, R. D. D.: Tectonothermal evolution of the Badajoz-Córdoba shear
1311 zone (SW Iberia): characteristics and $^{40}\text{Ar}/^{39}\text{Ar}$ mineral age constraints, *Tectonophysics*,
1312 231(1–3), 195–213, doi:10.1016/0040-1951(94)90130-9, 1994.
- 1313 Quesada, C., Braid, J. A., Fernandes, P., Ferreira, P., Jorge, R. S., Matos, J. X., Murphy, J. B.,
1314 Oliveira, J. T., Pedro, J. and Pereira, Z.: SW Iberia Variscan Suture Zone: Oceanic Affinity



- 1315 Units, in *The Geology of Iberia: A Geodynamic Approach*, edited by C. Quesada and J. T.
1316 Oliveira, pp. 131–171, Springer International Publishing, Cham., 2019.
- 1317 Rankin, D. W.: Appalachian salients and recesses: Late Precambrian continental breakup and
1318 the opening of the Iapetus Ocean, *J. Geophys. Res.* 1896-1977, 81(32), 5605–5619,
1319 doi:10.1029/JB081i032p05605, 1976.
- 1320 Ribeiro, A., Munhá, J., Dias, R., Mateus, A., Pereira, E., Ribeiro, L., Fonseca, P., Araújo, A.,
1321 Oliveira, T., Romão, J., Chaminé, H., Coke, C. and Pedro, J.: Geodynamic evolution of the SW
1322 Europe Variscides, *Tectonics*, 26(6), doi:10.1029/2006TC002058, 2007.
- 1323 Ries, A. C. and Shackleton, R. M.: Catanzonal Complexes of North-West Spain and North
1324 Portugal, Remnants of a Hercynian Thrust Plate, *Nat. Phys. Sci.*, 234(47), 65–68,
1325 doi:10.1038/physci234065a0, 1971.
- 1326 Ries, A. C. and Shackleton, R. M.: Patterns of Strain Variation in Arcuate Fold Belts, *Philos.*
1327 *Trans. R. Soc. Lond. Ser. Math. Phys. Sci.*, 283(1312), 281–288, 1976.
- 1328 Rodríguez-Cañero, R., Jabaloy-Sánchez, A., Navas-Parejo, P., Martín-Algarra, A., Rodríguez,
1329 R., Antonio, C., Sánchez, J., Navas, P., Agustín, P. and Algarra, M.: Linking Palaeozoic
1330 palaeogeography of the Betic Cordillera to the Variscan Iberian Massif : new insight through the
1331 first conodonts of the Nevado-Filábride Complex, *Int. J. Earth Sci.*, 107(5), 1791–1806,
1332 doi:10.1007/s00531-017-1572-8, 2018.
- 1333 Rosenbaum, G.: Geodynamics of oroclinal bending: Insights from the Mediterranean, *J.*
1334 *Geodyn.*, 82, 5–15, doi:10.1016/j.jog.2014.05.002, 2014.
- 1335 Rubio Pascual, F. J., Arenas, R., Martínez Catalán, J. R., Rodríguez Fernández, L. R. and
1336 Wijbrans, J. R.: Thickening and exhumation of the Variscan roots in the Iberian Central System:
1337 Tectonothermal processes and 40Ar/39Ar ages, *Tectonophysics*, 587, 207–221,
1338 doi:10.1016/j.tecto.2012.10.005, 2013.
- 1339 Rubio Pascual, F. J., López-Carmona, A. and Arenas, R.: Thickening vs. extension in the
1340 Variscan belt: P–T modelling in the Central Iberian autochthon, *Tectonophysics*, 681, 144–158,
1341 doi:10.1016/j.tecto.2016.02.033, 2016.
- 1342 Sánchez-García, T., Chichorro, M., Solá, A. R., Álvaro, J. J., Díez-Montes, A., Bellido, F.,
1343 Ribeiro, M. L., Quesada, C., Lopes, J. C., Dias da Silva, Í., González-Clavijo, E., Gómez
1344 Barreiro, J. and López-Carmona, A.: The Cambrian-Early Ordovician Rift Stage in the
1345 Gondwanan Units of the Iberian Massif, in *The Geology of Iberia: A Geodynamic Approach*,
1346 edited by C. Quesada and J. T. Oliveira, pp. 27–74, Springer International Publishing, Cham.,
1347 2019.
- 1348 Schulz, G.: *Descripción geológica de Asturias: Publicada de Real Orden. Con un atlas*, José
1349 Gonzalez., 1858.
- 1350 Schwartz, S. Y. and Vandervoo, R.: PALEOMAGNETIC EVALUATION OF THE OROCLINE
1351 HYPOTHESIS IN THE CENTRAL AND SOUTHERN APPALACHIANS, *Geophys. Res. Lett.*,
1352 10(7), 505–508, 1983.
- 1353 Shaw, J. and Johnston, S. T.: Terrane wrecks (coupled oroclinal) and paleomagnetic inclination



- 1354 anomalies, *Earth-Sci. Rev.*, 154, 191–209, doi:10.1016/j.earscirev.2016.01.003, 2016.
- 1355 Shaw, J., Johnston, S. T., Gutiérrez-Alonso, G. and Weil, A. B.: Oroclines of the Variscan
1356 orogen of Iberia: Paleocurrent analysis and paleogeographic implications, *Earth Planet. Sci.*
1357 *Lett.*, 329–330, 60–70, doi:10.1016/j.epsl.2012.02.014, 2012.
- 1358 Shaw, J., Johnston, S. T., Gutiérrez-Alonso, G. and Pastor-Galán, D.: Provenance variability
1359 along the Early Ordovician north Gondwana margin: Paleogeographic and tectonic implications
1360 of U-Pb detrital zircon ages from the Armorican Quartzite of the Iberian Variscan belt, *Bull. Geol.*
1361 *Soc. Am.*, 126(5–6), 702–719, doi:10.1130/B30935.1, 2014.
- 1362 Shaw, J., Johnston, S. T. and Gutiérrez-Alonso, G.: Orocline formation at the core of Pangea: A
1363 structural study of the Cantabrian orocline, NW Iberian Massif, *Lithosphere*, 7(6), 653–661,
1364 doi:10.1130/L461.1, 2015.
- 1365 Shaw, J., Johnston, S. T. and Gutiérrez-Alonso, G.: Orocline formation at the core of Pangea: A
1366 structural study of the Cantabrian orocline, NW Iberian Massif, *Lithosphere*, 8(1), 97–97,
1367 doi:10.1130/L461.1, 2016.
- 1368 Silva, Í. D. D., Valverde-Vaquero, P., González-Clavijo, E., Díez-Montes, A. and Catalán, J. R.
1369 M.: Structural and stratigraphical significance of U–Pb ages from the Mora and Saldanha
1370 volcanic complexes (NE Portugal, Iberian Variscides), *Geol. Soc. Lond. Spec. Publ.*, 405(1),
1371 115–135, doi:10.1144/SP405.3, 2014.
- 1372 Simancas, J. F., Carbonell, R., Lodeiro, F. G., Estaun, A., Juhlin, C., Ayarza, P., Kashubin, A.,
1373 Azor, A., Poyatos, D. M., Almodovar, G. R., Pascual, E., Saez, R. and Exposito, I.: Crustal
1374 structure of the transpressional Variscan orogen of SW Iberia: SW Iberia deep seismic reflection
1375 profile (IBERSEIS), *Tectonics*, 22(6), 25–25, 2003.
- 1376 Simancas, J. F., Ayarza, P., Azor, a., Carbonell, R., Martínez Poyatos, D., Pérez-Estaún, a. and
1377 González Lodeiro, F.: A seismic geotraverse across the Iberian Variscides: Orogenic
1378 shortening, collisional magmatism, and orocline development, *Tectonics*, 32(i), n/a-n/a,
1379 doi:10.1002/tect.20035, 2013.
- 1380 Solís-Alulima, B. E., López-Carmona, A., Gutiérrez Alonso, G. and Álvarez Valero, A. M.:
1381 Petrologic and thermobarometric study of the Riás schists (NW Iberian Massif), *Bol. Geológico*
1382 *Min.*, 130(3), 445–464, doi:10.21701/bolgeomin.130.3.004, 2019.
- 1383 Stampfli, G. M. and Borel, G. D.: The TRANSMED Transects in Space and Time: Constraints
1384 from Paleotectonic Evolution of the Mediterranean Domain., edited by W. Cavazza, F. M.
1385 Roure, W. Spakman, G. M. Stampfli, and P. A. Ziegler, pp. 53–80, Springer, Berlin., 2004.
- 1386 Stampfli, G. M., Hochard, C., Vèrard, C., Wilhem, C. and VonRaumer, J.: The Formation of
1387 Pangea, *Tectonophysics*, 593, 1–19, doi:10.1016/j.tecto.2013.02.037, 2013.
- 1388 Staub, R.: Gedanken zur Tektonik Spaniens., Zürich., 1926.
- 1389 Stewart, S. A.: Paleomagnetic analysis of fold kinematics and implications for geological models
1390 of the Cantabrian/Asturian arc, north Spain, *J. Geophys. Res. Solid Earth*, 100(B10), 20079–
1391 20094, doi:10.1029/95JB01482, 1995.



- 1392 Tait, J. A., Bachtadse, V. and Soffel, H. C.: Eastern Variscan fold belt : Paleomagnetic evidence
1393 for oroclinal bending, *Geology*, 24, 871–874, doi:10.1130/0091-7613(1996)024<0871, 1996.
- 1394 Tauxe, L.: *Essentials of Paleomagnetism*, Univ of California Press., 2010.
- 1395 Thomas, W. A.: Evolution of Appalachian-Ouachita Salients and Recesses from Reentrants and
1396 Promontories in the Continental Margin, *Am. J. Sci.*, 277(10), 1233–1278,
1397 doi:10.2475/ajs.277.10.1233, 1977.
- 1398 Thomas, W. A.: Genetic relationship of rift-stage crustal structure, terrane accretion, and
1399 foreland tectonics along the southern Appalachian-Ouachita orogen, *J. Geodyn.*, 37(3), 549–
1400 563, doi:10.1016/j.jog.2004.02.020, 2004.
- 1401 Tohver, E., Weil, A. B. B. B., Solum, J. G. G. G. and Hall, C. M. M. M.: Direct dating of
1402 carbonate remagnetization by $^{40}\text{Ar}/^{39}\text{Ar}$ analysis of the smectite–illite transformation, *Earth
1403 Planet. Sci. Lett.*, 274(3–4), 524–530, doi:10.1016/j.epsl.2008.08.002, 2008.
- 1404 Toit, A. L. Du: *Our wandering continents: an hypothesis of continental drifting*, Oliver and Boyd.
1405 [online] Available from: <http://books.google.es/books?id=iDZEAAAIAAJ>, 1937.
- 1406 Valladares, M. I., Barba, P., Ugidos, J. M., Colmenero, J. R. and Armenteros, I.: Upper
1407 Neoproterozoic-Lower Cambrian sedimentary successions in the Central Iberian Zone (Spain):
1408 sequence stratigraphy, petrology and chemostratigraphy. Implications for other European
1409 zones, *Int. J. Earth Sci.*, 89(1), 2–20, 2000.
- 1410 Van der Voo, R.: Paleomagnetism, oroclinal, and growth of the continental crust, *GSA Today*,
1411 14(12), 4–9, doi:10.1130/1052-5173(2004), 2004.
- 1412 Vergés, J.: Estudio del Complejo volcánico-sedimentario del Devónico y de la estructura de la
1413 terminación oriental del sinclinal de Almadén (Ciudad Real), in *Libro Jubilar JM Rios. Tomo 3*,
1414 pp. 215–229., 1983.
- 1415 Vissers, R. L. M., van Hinsbergen, D. J. J., van der Meer, D. G. and Spakman, W.: Cretaceous
1416 slab break-off in the Pyrenees: Iberian plate kinematics in paleomagnetic and mantle reference
1417 frames, *Gondwana Res.*, 34, 49–59, doi:10.1016/J.GR.2016.03.006, 2016.
- 1418 van der Voo, R., Stamatakos, J. A. and Pares, J. M.: Kinematic constraints on thrust-belt
1419 curvature from syndeformational magnetizations in the Lagos del Valle Syncline in the
1420 Cantabrian Arc, Spain, *J. Geophys. Res.-Solid Earth*, 102(B5), 10105–10119, 1997.
- 1421 Weil, A., Pastor-Galán, D., Johnston, S. T. and Gutiérrez-Alonso, G.: Late/Post Variscan
1422 Orocline Formation and Widespread Magmatism, in *The Geology of Iberia: A Geodynamic
1423 Approach*, edited by C. Quesada and J. T. Oliveira, pp. 527–542, Springer International
1424 Publishing, Cham., 2019.
- 1425 Weil, A. B.: Kinematics of orocline tightening in the core of an arc: Paleomagnetic analysis of
1426 the Ponga Unit, Cantabrian Arc, northern Spain, *Tectonics*, 25(3), n/a-n/a,
1427 doi:10.1029/2005TC001861, 2006.
- 1428 Weil, A. B. and Sussman, A. J.: Classifying curved orogens based on timing relationships
1429 between structural development and vertical-axis rotations, vol. 383, edited by A. J. Sussman



- 1430 and A. B. Weil, pp. 1–16, Geological Society of America., 2004.
- 1431 Weil, A. B., Van der Voo, R., van der Pluijm, B. A. and Parés, J. M.: The formation of an orocline
1432 by multiphase deformation: a paleomagnetic investigation of the Cantabria–Asturias Arc
1433 (northern Spain), *J. Struct. Geol.*, 22(6), 735–756, doi:10.1016/S0191-8141(99)00188-1, 2000.
- 1434 Weil, A. B., van der Voo, R. and van der Pluijm, B. A.: Oroclinal bending and evidence against
1435 the Pangea megashear: The Cantabria-Asturias arc (northern Spain), *Geology*, 29(11), 991–
1436 994, 2001.
- 1437 Weil, A. B., Van der Voo, R. and Voo, R. V. D.: Insights into the mechanism for orogen-related
1438 carbonate remagnetization from growth of authigenic Fe-oxide: A scanning electron microscopy
1439 and rock magnetic study of Devonian carbonates from northern Spain, *J. Geophys. Res.-Solid
1440 Earth*, 107(B4), 14–14, 2002.
- 1441 Weil, A. B., Gutiérrez-Alonso, G. and Conan, J.: New time constraints on lithospheric-scale
1442 oroclinal bending of the Ibero-Armorican Arc: a palaeomagnetic study of earliest Permian rocks
1443 from Iberia, *J. Geol. Soc.*, 167(1), 127–143, doi:10.1144/0016-76492009-002, 2010.
- 1444 Weil, A.B., Yonkee, A., and Sussman, A.: Reconstructing the kinematics of thrust sheet rotation:
1445 a paleomagnetic study of Triassic redbeds from the Wyoming Salient, U.S.A., *GSA Bulletin*,
1446 122, ½ 2-23, 2010.
- 1447 Weil, A. B. B., Gutiérrez-Alonso, G., Johnston, S. T. and Pastor-Galán, D.: Kinematic
1448 constraints on buckling a lithospheric-scale orocline along the northern margin of Gondwana: A
1449 geologic synthesis, *Tectonophysics*, 582, 25–49, doi:10.1016/j.tecto.2012.10.006, 2013.
- 1450 Woodcock, N. H., Soper, N. J. and Strachan, R. A.: A Rheic cause for the Acadian deformation
1451 in Europe, *J. Geol. Soc.*, 164, 1023–1036, 2007.
- 1452 Yenes, M., Alvarez, F. and Gutierrez-Alonso, G.: Granite emplacement in orogenic
1453 compressional conditions: the La Alberca-Bejar granitic area (Spanish Central System, Variscan
1454 Iberian Belt), *J. Struct. Geol.*, 21(10), 1419–1440, 1999.
- 1455 Yonkee, A., Weil, A.B., and Sussman, A.: Reconstructing the kinematic evolution of curved
1456 mountain belts: internal strain patterns in the Wyoming Salient, Sevier thrust belt, U.S.A., *GSA
1457 Bulletin*, 122, ½, 24-50, 2010.
- 1458 Yonkee, A. and Weil, A. B.: Quantifying vertical axis rotation in curved orogens: Correlating
1459 multiple data sets with a refined weighted least squares strike test, *Tectonics*, 29(3), 31 PP.-31
1460 PP., doi:10.1029/2008TC002312, 2010b.
- 1461 Zegers, T. E., Dekkers, M. J. and Bailly, S.: Late Carboniferous to Permian remagnetization of
1462 Devonian limestones in the Ardennes: Role of temperature, fluids, and deformation, *J. Geophys.
1463 Res. Solid Earth*, 108(B7), n/a-n/a, doi:10.1029/2002JB002213, 2003.

1464 Captions

- 1465 Fig. 1 Simplified paleogeographic map of the Variscan-Alleghanian orogeny prior to the
1466 Jurassic break-up of Pangea, with the major orogenic curves labeled. Note, this map represents



1467 Iberian outcrops without taking account of the post Jurassic Alpine deformation (see text for
1468 details e.g. Gong et al., 2008; Pastor-Galán et al., 2018). Slightly darker colors in the Variscan
1469 belt indicate present-day European and African outcrops (modified after Martínez-Catalán et al.,
1470 2009; Weil et al., 2013).

1471 Fig. 2 A) Present-day configuration of the tectonostratigraphic zones of the Iberian
1472 Variscides and its major structures. White areas represent Mesozoic and Cenozoic cover. B)
1473 Three competing geometric proposals for the Central Iberian curve. 1) A disharmonic curvature,
1474 up to 160° at the outer arc but much less pronounced at the inner arc (Aerden, 2004); 2) A
1475 harmonic, but more open curvature as suggested by Martínez Catalán (2012); 3) an isoclinal
1476 curvature model (Shaw et al., 2012). C) Distribution of the E1 (in migmatitic domes) and C3 to
1477 post-C3 granitoids in the NW of Iberia (modified from Pastor-Galán et al., 2016)

1478 Fig. 3 A) Stratigraphic synthesis of the Gondwanan platform series in NW Iberia.
1479 Cantabrian Zone columns are after Aramburu et al., 2002; Bastida, 2004; Murphy et al 2008;
1480 Pastor-Galán et al., 2013a; 2013b. Iberian Range follows Gozalo et al., 2008; Mergl and
1481 Zamora, 2012 and Calvín and Casas, 2014. West Asturian Leonese Zone stratigraphy is after
1482 Pérez-Estaún, 1990; Marcos, 2004; Martínez-Catalán et al., 2004a; Gutiérrez-Marco et al.,
1483 2019. Central Iberian Zone follows Díez-Balda, 1986; Valladares et al., 2000; Díez Montes,
1484 2007; Martínez-Catalán et al., 2004b; del Moral and Sarmiento, 2008; García-Arias et al., 2018.
1485 B) Ordovician paleocurrents orientations, modified from Shaw et al., 2012. C) Schematic basin
1486 architecture inferred from the stratigraphic compilation.

1487 Fig. 4 A) The kinematic evolution of the Cantabrian Orocline in its core, the Cantabrian
1488 Zone, inferred from total least squares (TLS) orocline tests (Pastor-Galán et al. 2017). B) Shows
1489 three orocline (strike) tests used to constrain the kinematics of the Cantabrian Orocline. The
1490 Ordovician paleocurrents, which predate any orogenic movement, recorded the complete
1491 vertical-axis rotation history and yields a slope (m) of ~ 1 . The Moscovian paleomagnetic data
1492 (from Weil et al., 2013; Pmag.), which postdates the main orogenic phases (C1, C2 and E1) and
1493 is coeval with C3, shows a slope of ~ 1 . The Gzhelian joint sets (from Pastor-Galán et al., 2011)
1494 orocline test shows a slope of ~ 0.5 , which indicates that half of the orocline was already formed
1495 at ~ 304 Ma.

1496 Fig. 5 A) Aeromagnetic map of Spain (Ardizzone et al., 1989, for Spain and the World
1497 Digital Magnetic Anomaly Map (WDMAM project) and Portugal (modified from Martínez Catalán,
1498 2012 and Martínez Catalán et al., 2015), showing the possible trace of the Central Iberian
1499 curve. B) Bouguer anomalies of the Iberian Peninsula, modified from Ayala et al., 2016. Gravity
1500 anomalies do not reflect the geometry of the Cantabrian Orocline nor the Central Iberian curve



1501 but are related to the Cenozoic Alpine lithospheric structure.

1502 Fig. 6 Paleomagnetic studies related to the Cantabrian Orocline and the Central Iberian
1503 curve: (1) Synthesis of paleomagnetism in the core of the Cantabrian Orocline (see Weil et al.,
1504 2013); (2) Permian (eP) components synthesized in Weil et al. (2010); (3) Ordovician volcanics
1505 and limestones (Laquiana) in the boundary between the West Asturian-Leonese and Central
1506 Iberian Zones (Fernández-Lozano et al., 2016); (4) Devonian sedimentary sequences and
1507 Permian subvolcanics in the Iberian ranges (Pastor-Galán et al., 2018); (5) Permian dykes and
1508 sills (Calvín et al., 2014); (5) Anatectic granites (E1) and mantle derived granitoids (C3) from
1509 Tormes Dome and Central System (Pastor-Galán et al., 2016); (6) Cambrian limestones from
1510 Tamames (N) and los Navalucillos (S) (Pastor-Galán et al., 2015a); (7) Ediacaran-Early
1511 Cambrian sedimentary rocks in the southern sector of the Central Iberian Zone (Pastor-Galán et
1512 al., 2017b); (8) Almadén volcanics from the Central Iberian Zone (Perroud et al., 1991; Parés
1513 and van der Voo, 1992; Leite Mendes et al. in press) and Volcanic rocks from southern Ossa
1514 Morena and the South Portuguese Zone (Leite Mendes et al. in press)

1515 Fig. 7 Magnetization components with a positive reversal test in the extensional
1516 anatectic granites of Tormes (A) and Martinamor Domes (B). This component is interpreted as
1517 primary with a magnetization age of >318 Ma (Pastor-Galán et al., 2016). C) Distribution of
1518 directions and VGPs and statistical parameters from both domes combined.

1519 Fig. 8 Cartoon depicting the different vertical axis rotation events that occurred in the
1520 Cantabrian Zone and the Iberian Range, modified from Pastor-Galán et al. (2018). (A) Original
1521 quasilinear Variscan Orogenic belt, B) Formation of the Cantabrian Orocline around the
1522 Carboniferous–Permian boundary after a $\sim 70^\circ$ counterclockwise rotation in the Southern branch
1523 of the Cantabrian Zone and the Iberian Range. This rotation matches the rotation for the
1524 Cantabrian Orocline, see the fit of the Iberian Range Component #2 in the orocline test for the
1525 Cantabrian Zone (below). C) Post Permian (Cenozoic) rotation of $\sim 22^\circ$ clockwise (CW) likely
1526 produced by differential shortening during the Alpine orogeny (Izquierdo-Llavall et al., 2018).
1527 Below, the global magnetic polarity time scale for the Pennsylvanian and Cisuralian (following
1528 Ogg et al., 2016). TLS = Total Least Squares. Note that once the 22° CW rotation in the Iberian
1529 Range is corrected, components #2, #1, and P fit as expected with the APWP for the southern
1530 limb of the orocline (Pastor-Galán et al., 2016).

1531 Fig. 9 Compilation of the directional distributions and average declinations with
1532 parachute of confidence (Δ Declination) in sites around the Central Iberian curve (see Fig. 6).
1533 The results show general CCW rotations in contrast to the expected CW if the Central Iberia
1534 curve formed by vertical-axis rotations (see text). Results are compared with the expected



1535 declinations if those sites were part of the Cantabrian Orocline following the methodology
1536 described in Pastor-Galán et al., 2017b.

1537 Fig. 10 Orocline test of the Cantabrian Orocline (Weil et al., 2013) compared with the
1538 magnetizations found in the adjacent Laurussian segments of the orogen: Ireland (Pastor-Galán
1539 et al., 2015b) and the South Portuguese Zone (Leite Mendes et al., in press)

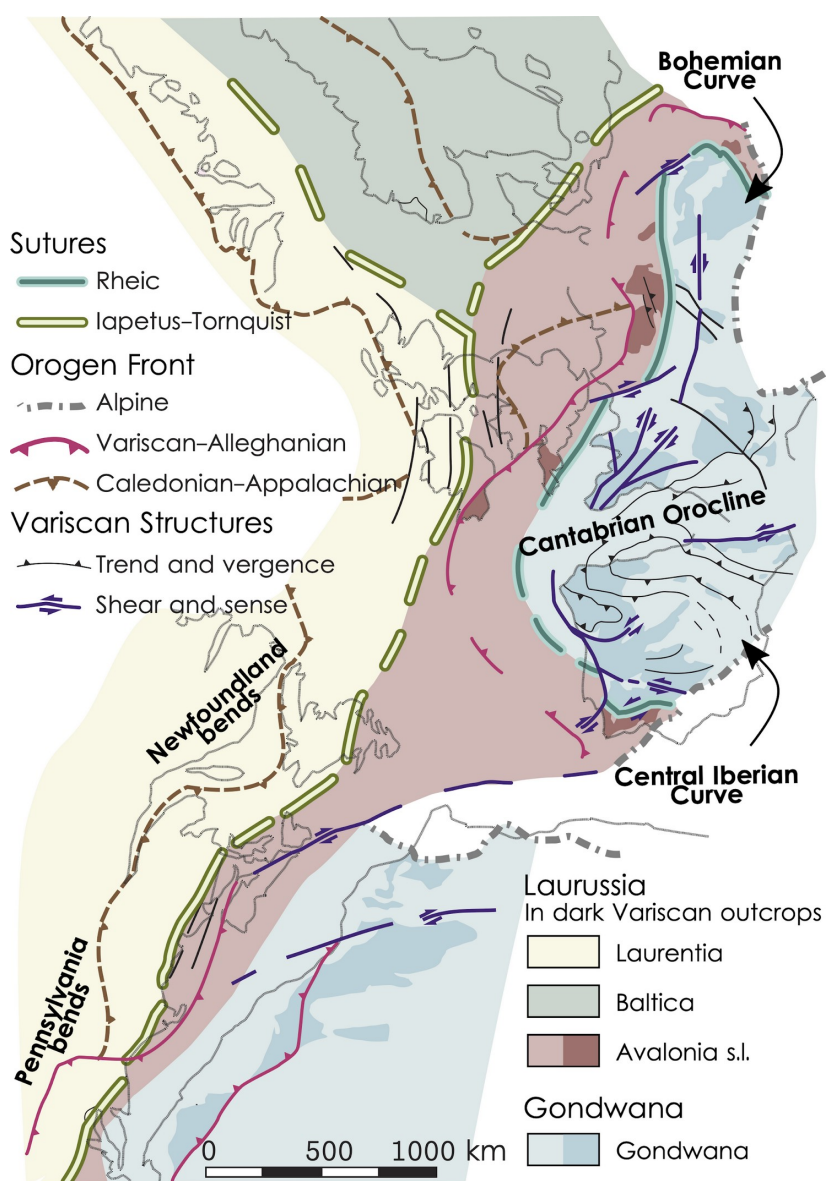
1540 Fig. 11 Structural analysis of mullions in the Central Iberian Zone (after Pastor-Galán et
1541 al., 2019b) A) Photograph (with card scale, 10cm) of a bedding plane surface showing the
1542 mullions and photograph analysis. B) Interpretation of the outcrop with fold axis traces depicting
1543 the deformation phase responsible for each structure. C) Result of retro-deformation of mullions
1544 in the Mogadouro road section modified from Pastor-Galán et al. (2019b). Unfolding the effects
1545 of D3 on D2 mullions. Unfolding the effects of C3 and E1 in C1 mullions.

1546 Fig. 12 Pionering hypothesis for the Central Iberian curve. Note that none of them fulfill
1547 the most recent geometric and kinematic criteria. A) Simplified ribbon continent model after
1548 Johnston et al. (2013) and Shaw and Johnston (2016). B) Dextral mega-shear model from
1549 Martínez-Catalán (2011). C) Kinematic model with indentation and left-lateral shearing after
1550 Simancas et al. (2013)

1551 Fig. 13 Preliminary kinematic proposal for the Iberian Variscides. A) Pre-collisional stage
1552 after the opening of the Galicia Tras-os-Montes restricted seaway (e.g. Pin et al., 2002;
1553 Gutiérrez-Alonso et al., 2008a; Arenas et al., 2016). The irregular shape of the margin and the
1554 younging westwards deformation front (e.g. Daleyer et al., 1997) resulted in tectonic escape
1555 towards the still open Rheic Ocean (e.g. Braid et al., 2011; Murphy et al., 2016). B) After closure
1556 of the Rheic ocean, C1 and C2 structures formed. The Galicia Tras-os-Montes was emplaced
1557 orogen parallel (e.g. Martínez-Catalán et al., 1990; Dias da Silva et al., in press), preserving the
1558 shape of the seaway, i.e. a primary arc. C) The gravitational collapse of the orogen produced
1559 widespread anatexis and folding interference in the hinterland and the emplacement of the
1560 foreland fold-and-thrust belt. D) At Pennsylvanian times a change in the far-field stress buckled
1561 the Variscan belt around a vertical axis (see Gutiérrez-Alonso et al., 2008; Weil et al., 2013;
1562 Pastor-Galán et al., 2015a for details), creating new interference patterns and a lithospheric
1563 scale response (see Gutiérrez-Alonso et al., 2004, 2011a; Pastor-Galán et al., 2012a). E) When
1564 the orocline became too tight to keep rotating, new cross-cutting brittle structures (C4) formed
1565 and minor extensional collapse (E2) occurred (e.g. Fernández-Lozano et al., 2019; Dias da
1566 Silva et al., in press).

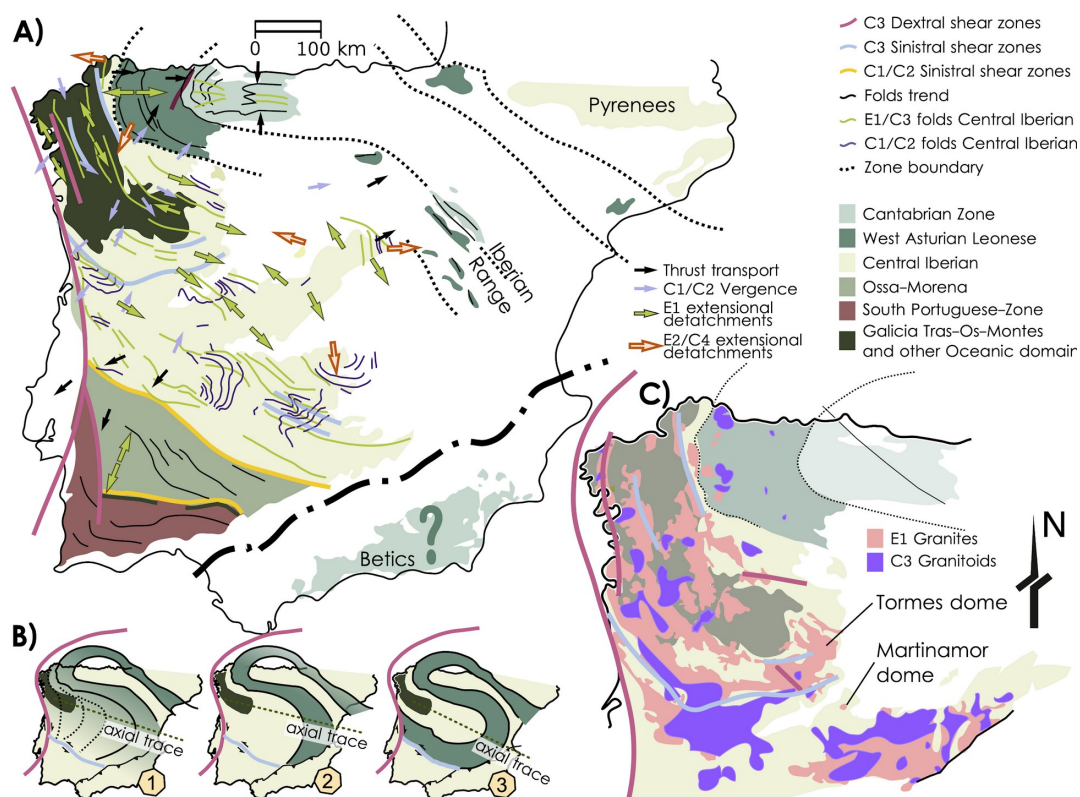


1567 Fig. 1 Simplified paleogeographic map of the Variscan-Alleghanian orogeny prior to the
1568 Jurassic break-up of Pangea, with the major orogenic curves labeled. Note, this map represents
1569 Iberian outcrops without taking account of the post Jurassic Alpine deformation (see text for
1570 details e.g. Gong et al., 2008; Pastor-Galán et al., 2018). Slightly darker colors in the Variscan
1571 belt indicate present-day European and African outcrops (modified after Martínez-Catalán et al.,
1572 2009; Weil et al., 2013).



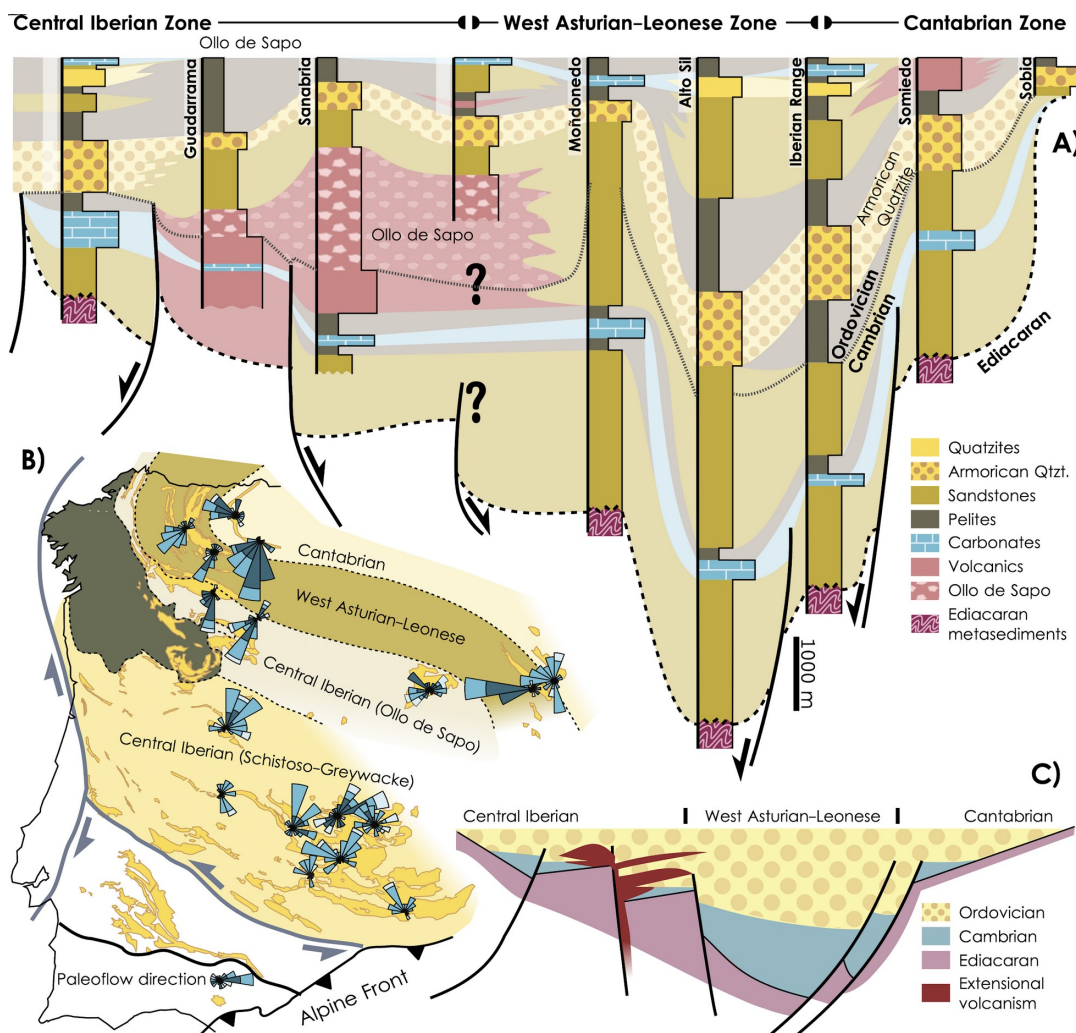


1573 Fig. 2 A) Present-day configuration of the tectonostratigraphic zones of the Iberian
 1574 Variscides and its major structures. White areas represent Mesozoic and Cenozoic cover. B)
 1575 Three competing geometric proposals for the Central Iberian curve. 1) A disharmonic curvature,
 1576 up to 160° at the outer arc but much less pronounced at the inner arc (Aerden, 2004); 2) A
 1577 harmonic, but more open curvature as suggested by Martínez Catalán (2012); 3) an isoclinal
 1578 curvature model (Shaw et al., 2012). C) Distribution of the E1 (in migmatitic domes) and C3 to
 1579 post-C3 granitoids in the NW of Iberia (modified from Pastor-Galán et al., 2016)



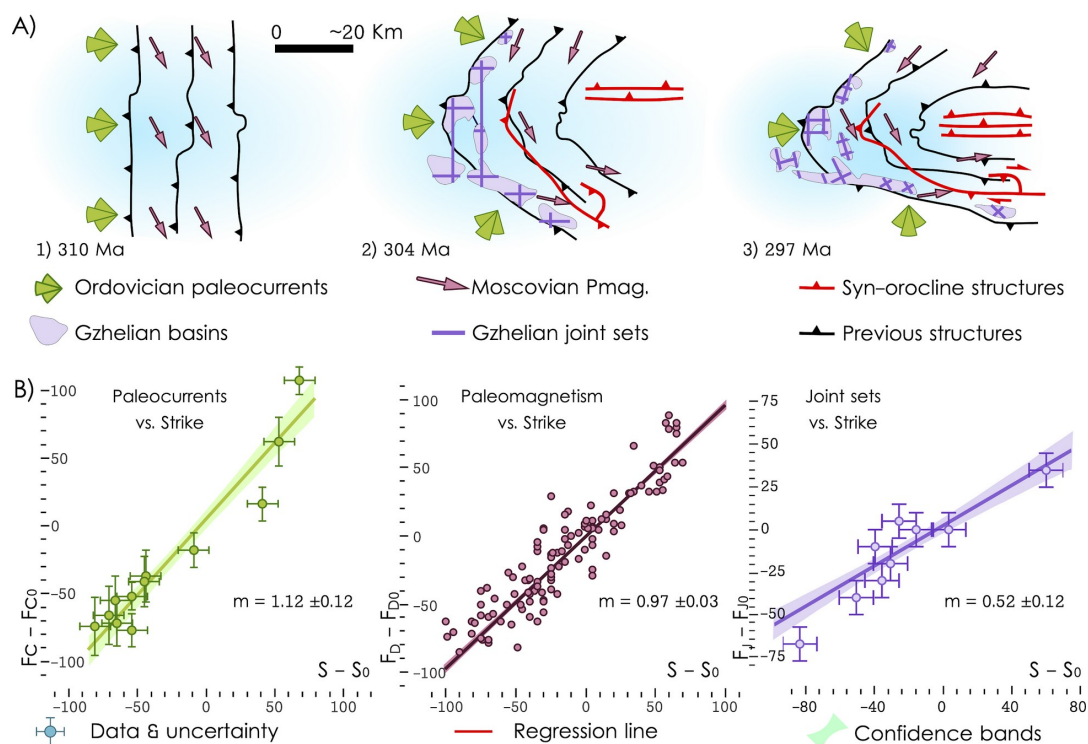


1580 Fig. 3 A) Stratigraphic synthesis of the Gondwanan platform series in NW Iberia.
 1581 Cantabrian Zone columns are after Aramburu et al., 2002; Bastida, 2004; Murphy et al 2008;
 1582 Pastor-Galán et al., 2013a; 2013b. Iberian Range follows Gozalo et al., 2008; Mergl and
 1583 Zamora, 2012 and Calvín and Casas, 2014. West Asturian Leonese Zone stratigraphy is after
 1584 Pérez-Estaún, 1990; Marcos, 2004; Martínez-Catalán et al., 2004a; Gutiérrez-Marco et al.,
 1585 2019. Central Iberian Zone follows Díez-Balda, 1986; Valladares et al., 2000; Díez Montes,
 1586 2007; Martínez-Catalán et al., 2004b; del Moral and Sarmiento, 2008; García-Arias et al., 2018.
 1587 B) Ordovician paleocurrents orientations, modified from Shaw et al., 2012. C) Schematic basin
 1588 architecture inferred from the stratigraphic compilation.



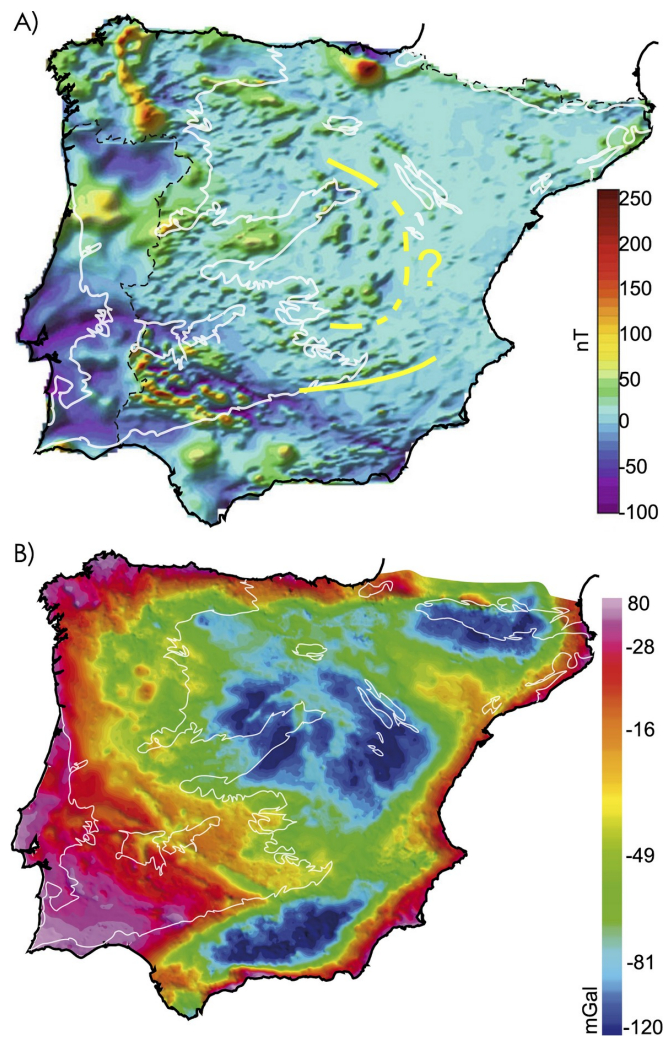


1589 Fig. 4 A) The kinematic evolution of the Cantabrian Orocline in its core, the Cantabrian
 1590 Zone, inferred from total least squares (TLS) orocline tests (Pastor-Galán et al. 2017). B) Shows
 1591 three orocline (strike) tests used to constrain the kinematics of the Cantabrian Orocline. The
 1592 Ordovician paleocurrents, which predate any orogenic movement, recorded the complete
 1593 vertical-axis rotation history and yields a slope (m) of ~ 1 . The Moscovian paleomagnetic data
 1594 (from Weil et al., 2013; Pmag.), which postdates the main orogenic phases (C1, C2 and E1) and
 1595 is coeval with C3, shows a slope of ~ 1 . The Gzhelian joint sets (from Pastor-Galán et al., 2011)
 1596 orocline test shows a slope of ~ 0.5 , which indicates that half of the orocline was already formed
 1597 at ~ 304 Ma.



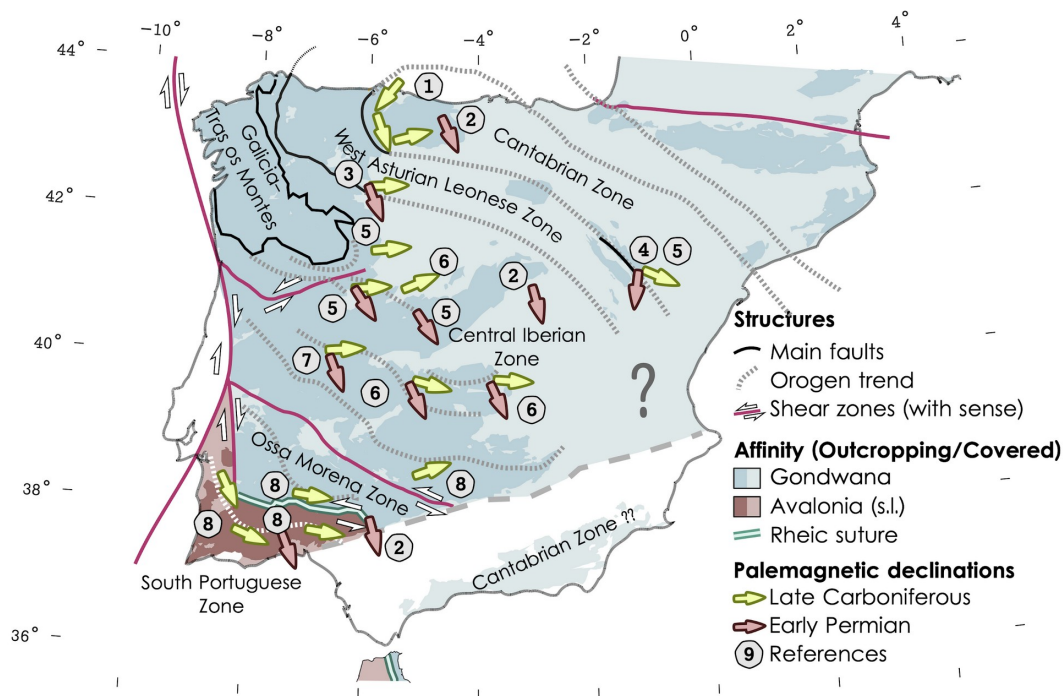


1598 Fig. 5 A) Aeromagnetic map of Spain (Ardizzone et al., 1989, for Spain and the World
1599 Digital Magnetic Anomaly Map (WDMAM project) and Portugal (modified from Martínez Catalán,
1600 2012 and Martínez Catalán et al., 2015), showing the possible trace of the Central Iberian
1601 curve. B) Bouguer anomalies of the Iberian Peninsula, modified from Ayala et al., 2016. Gravity
1602 anomalies do not reflect the geometry of the Cantabrian Orocline nor the Central Iberian curve
1603 but are related to the Cenozoic Alpine lithospheric structure.



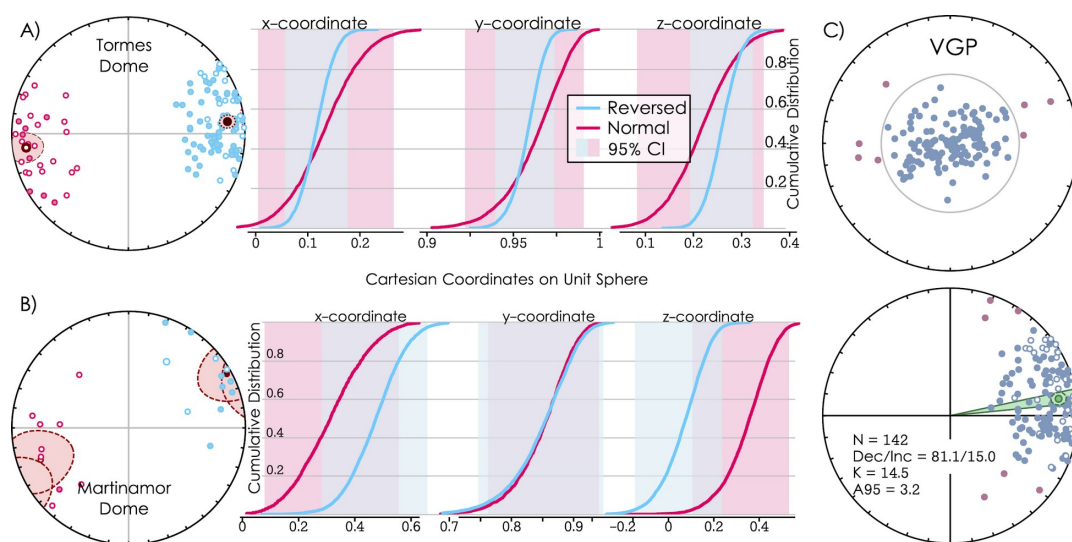


1604 Fig. 6 Paleomagnetic studies related to the Cantabrian Orocline and the Central Iberian
 1605 curve: (1) Synthesis of paleomagnetism in the core of the Cantabrian Orocline (see Weil et al.,
 1606 2013); (2) Permian (eP) components synthesized in Weil et al. (2010); (3) Ordovician volcanics
 1607 and limestones (Laquiana) in the boundary between the West Asturian-Leonese and Central
 1608 Iberian Zones (Fernández-Lozano et al., 2016); (4) Devonian sedimentary sequences and
 1609 Permian subvolcanics in the Iberian ranges (Pastor-Galán et al., 2018); (5) Permian dykes and
 1610 sills (Calvín et al., 2014); (5) Anatectic granites (E1) and mantle derived granitoids (C3) from
 1611 Tormes Dome and Central System (Pastor-Galán et al., 2016); (6) Cambrian limestones from
 1612 Tamames (N) and los Navalucillos (S) (Pastor-Galán et al., 2015a); (7) Ediacaran-Early
 1613 Cambrian sedimentary rocks in the southern sector of the Central Iberian Zone (Pastor-Galán et al.
 1614 al., 2017b); (8) Almadén volcanics from the Central Iberian Zone (Perroud et al., 1991; Parés
 1615 and van der Voo, 1992; Leite Mendes et al. in press) and Volcanic rocks from southern Ossa
 1616 Morena and the South Portuguese Zone (Leite Mendes et al, in press)



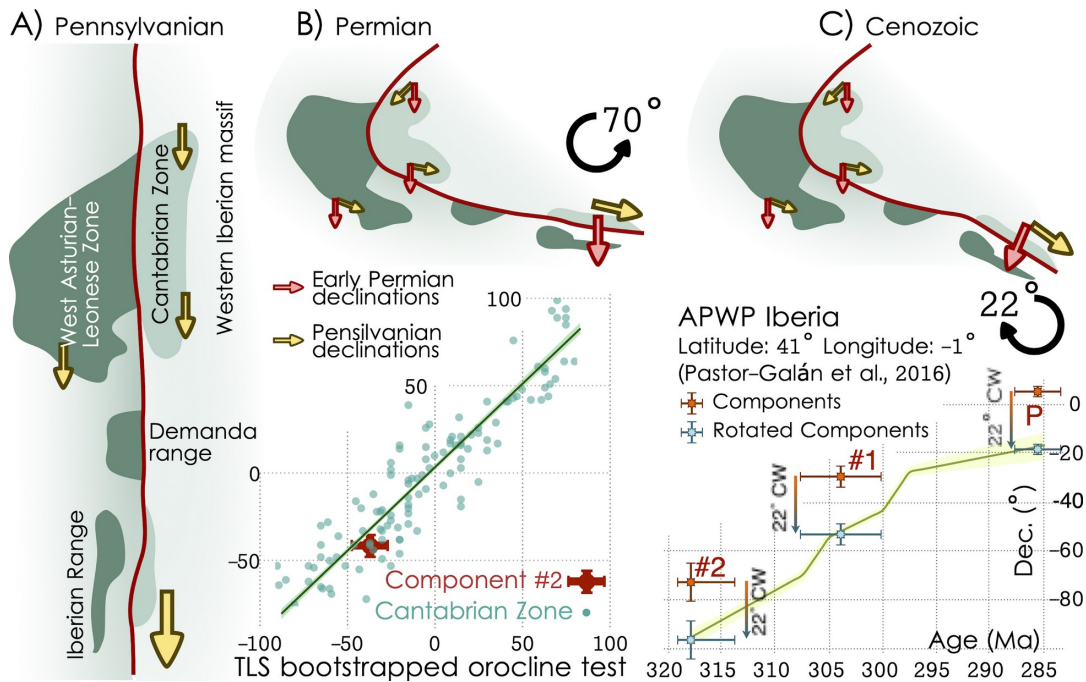


1617 Fig. 7 Magnetization components with a positive reversal test in the extensional anatectic
1618 granites of Tormes (A) and Martinamor Domes (B). This component is interpreted as primary
1619 with a magnetization age of >318 Ma (Pastor-Galán et al., 2016). C) Distribution of directions
1620 and VGPs and statistical parameters from both domes combined.



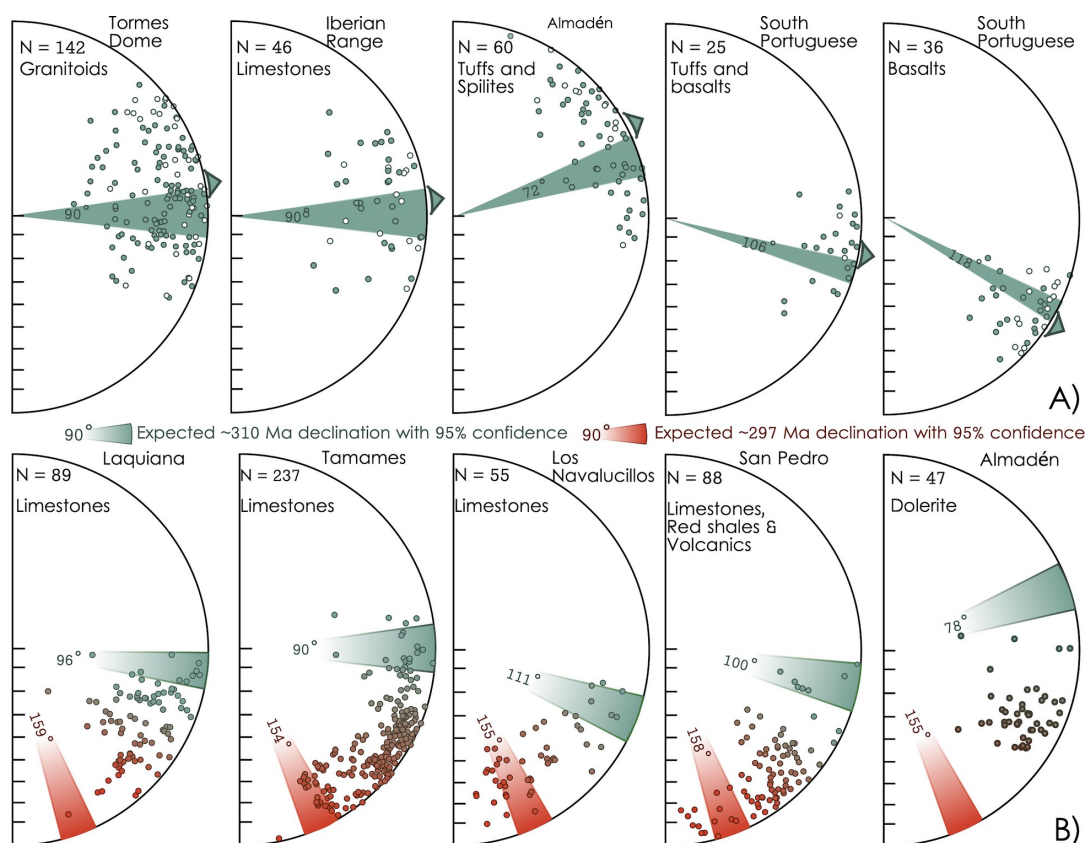


1621 Fig. 8 Cartoon depicting the different vertical axis rotation events that occurred in the
 1622 Cantabrian Zone and the Iberian Range, modified from Pastor-Galán et al. (2018). (A) Original
 1623 quasilinear Variscan Orogenic belt, B) Formation of the Cantabrian Orocline around the
 1624 Carboniferous–Permian boundary after a $\sim 70^\circ$ counterclockwise rotation in the Southern branch
 1625 of the Cantabrian Zone and the Iberian Range. This rotation matches the rotation for the
 1626 Cantabrian Orocline, see the fit of the Iberian Range Component #2 in the orocline test for the
 1627 Cantabrian Zone (below). C) Post Permian (Cenozoic) rotation of $\sim 22^\circ$ clockwise (CW) likely
 1628 produced by differential shortening during the Alpine orogeny (Izquierdo-Llavall et al., 2018).
 1629 Below, the global magnetic polarity time scale for the Pennsylvanian and Cisuralian (following
 1630 Ogg et al., 2016). TLS = Total Least Squares. Note that once the 22° CW rotation in the Iberian
 1631 Range is corrected, components #2, #1, and P fit as expected with the APWP for the southern
 1632 limb of the orocline (Pastor-Galán et al., 2016)



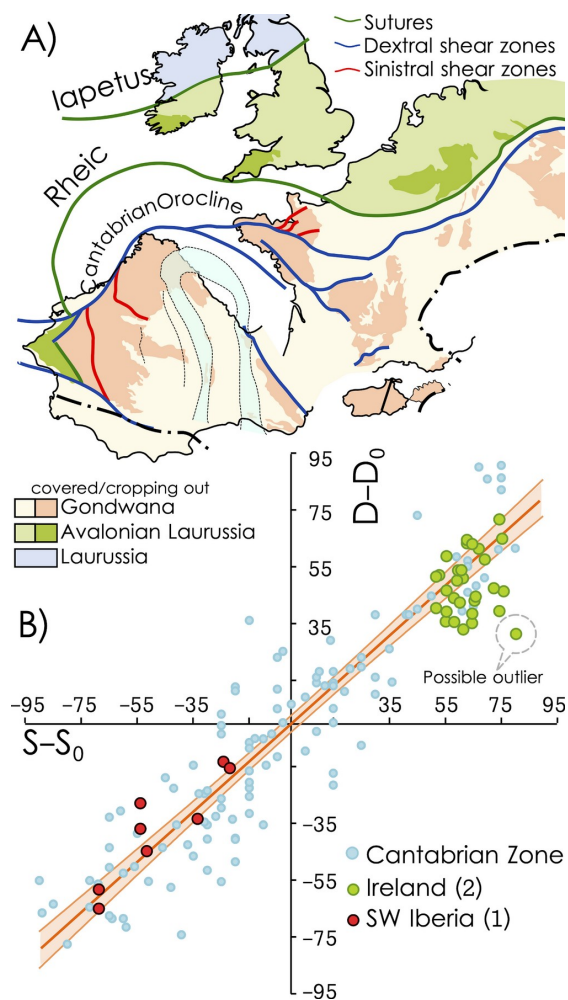


1633 Fig. 9 Compilation of the directional distributions and average declinations with parachute of
 1634 confidence (Δ Declination) in sites around the Central Iberian curve (see Fig. 6). The results
 1635 show general CCW rotations in contrast to the expected CW if the Central Iberia curve formed
 1636 by vertical-axis rotations (see text). Results are compared with the expected declinations if
 1637 those sites were part of the Cantabrian Orocline following the methodology described in Pastor-
 1638 Galán et al., 2017b



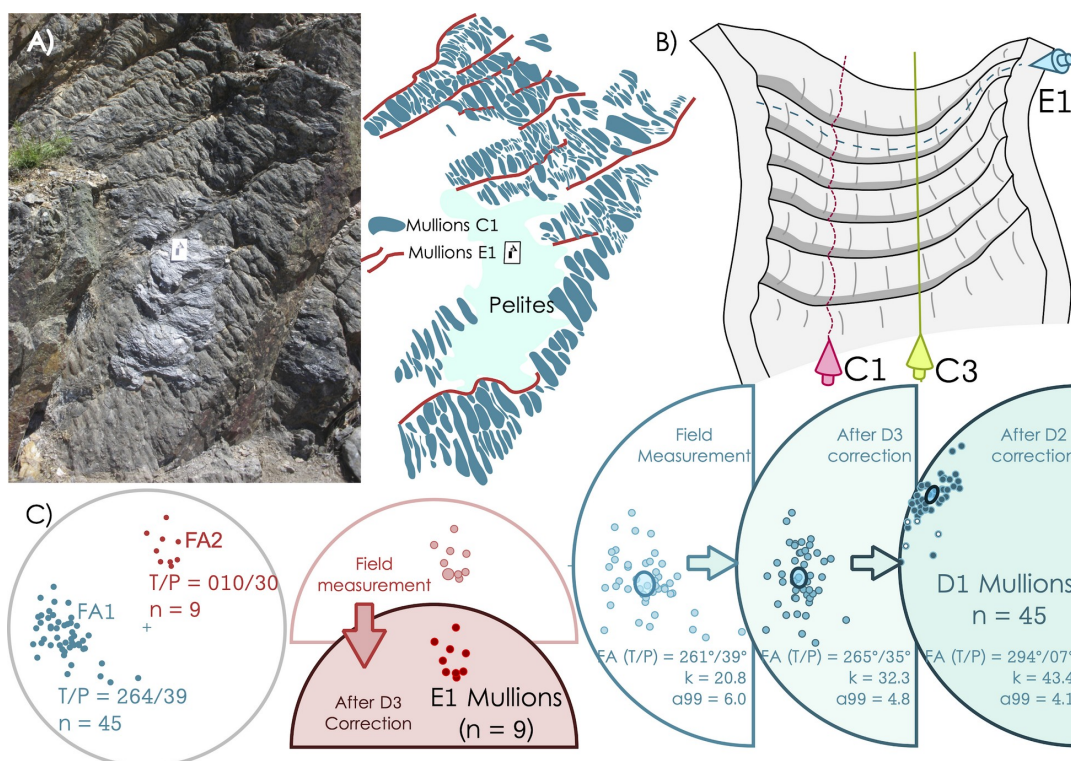


1639 Fig. 10 Orocline test of the Cantabrian Orocline (Weil et al., 2013) compared with the
1640 magnetizations found in the adjacent Laurussian segments of the orogen: Ireland (Pastor-Galán
1641 et al., 2015b) and the South Portuguese Zone (Leite Mendes et al., in press)



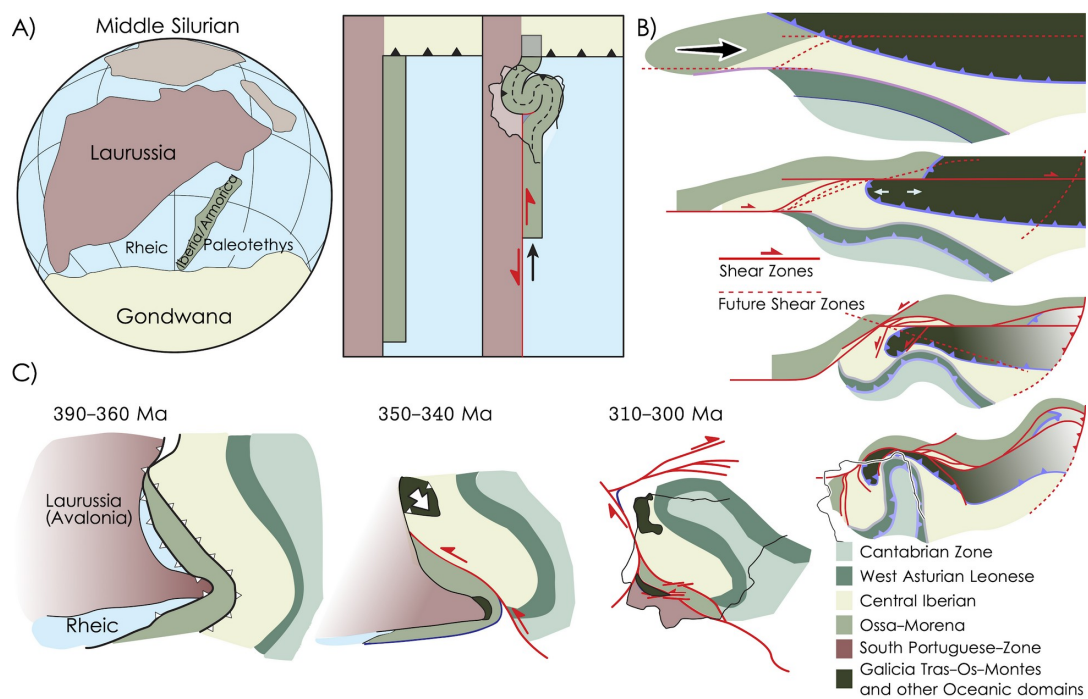


1642 Fig. 11 Structural analysis of mullions in the Central Iberian Zone (after Pastor-Galán et
 1643 al., 2019b) A) Photograph (with card scale, 10cm) of a bedding plane surface showing the
 1644 mullions and photograph analysis. B) Interpretation of the outcrop with fold axis traces depicting
 1645 the deformation phase responsible for each structure. C) Result of retro-deformation of mullions
 1646 in the Mogadouro road section modified from Pastor-Galán et al. (2019b). Unfolding the effects
 1647 of D3 on D2 mullions. Unfolding the effects of C3 and E1 in C1 mullions.





1648 Fig. 12 Pioneering hypothesis for the Central Iberian curve. Note that none of them fulfill
 1649 the most recent geometric and kinematic criteria. A) Simplified ribbon continent model after
 1650 Johnston et al. (2013) and Shaw and Johnston (2016). B) Dextral mega-shear model from
 1651 Martínez-Catalán (2011). C) Kinematic model with indentation and left-lateral shearing after
 1652 Simancas et al. (2013)





1653 Fig. 13 Preliminary kinematic proposal for the Iberian Variscides. A) Pre-collisional stage
1654 after the opening of the Galicia Tras-os-Montes restricted seaway (e.g. Pin et al., 2002;
1655 Gutiérrez-Alonso et al., 2008a; Arenas et al., 2016). The irregular shape of the margin and the
1656 younging westwards deformation front (e.g. Daleyer et al., 1997) resulted in tectonic escape
1657 towards the still open Rheic Ocean (e.g. Braid et al., 2011; Murphy et al., 2016). B) After closure
1658 of the Rheic ocean, C1 and C2 structures formed. The Galicia Tras-os-Montes was emplaced
1659 orogen parallel (e.g. Martínez-Catalán et al., 1990; Dias da Silva et al., in press), preserving the
1660 shape of the seaway, i.e. a primary arc. C) The gravitational collapse of the orogen produced
1661 widespread anatexis and folding interference in the hinterland and the emplacement of the
1662 foreland fold-and-thrust belt. D) At Pennsylvanian times a change in the far-field stress buckled
1663 the Variscan belt around a vertical axis (see Gutiérrez-Alonso et al., 2008; Weil et al., 2013;
1664 Pastor-Galán et al., 2015a for details), creating new interference patterns and a lithospheric
1665 scale response (see Gutiérrez-Alonso et al., 2004, 2011a; Pastor-Galán et al., 2012a). E) When
1666 the orocline became too tight to keep rotating, new cross-cutting brittle structures (C4) formed
1667 and minor extensional collapse (E2) occurred (e.g. Fernández-Lozano et al., 2019; Dias da
1668 Silva et al., in press).

